SMA 13701.05R003 (VOLUME VI)

MIDLAND SEISMIC MARGIN EARTHQUAKE
STRUCTURAL EVALUATION

BORATED WATER STORAGE TANK AND FOUNDATION

prepared for

CONSUMERS POWER COMPANY
Jackson, Michigan

November, 1982

STRUCTURAL MECHANICS ASSOCIATES
A Calif. Corp.
5160 Birch Street, Newport Beach, Calif. 92660 (714) 833-7552

SMA 13701.05R003(VOLUME VI)

MIDLAND SEISMIC MARGIN EARTHQUAKE STRUCTURAL EVALUATION

VOLUME VI

BORATED WATER STORAGE TANK AND FOUNDATION

by

Robert P. Kennedy
Stephen A. Short
Wen-How Tong

Approved: _____
R. P. Kennedy
President

Approved: _____
T. R. Kipp
Manager of
Quality Assurance

prepared for
CONSUMERS POWER COMPANY
Jackson, Michigan

November, 1982

STRUCTURAL MECHANICS ASSOCIATES
A Calif. Corp.

5100 Birch Street, Newport Beach, Calif. 92660 (714) 833-7552

REVISIONS

Document Number SMA 13701.05R003(Volume VI)

Title Midland Seismic Margin Earthquake Structural Evaluation Volume VI, Borated Water Storage Tank and Foundation

Rev.	Description	QA	Project Manager
4-30-82	Draft for Review	Thomas K. Kipp 4/30/82	D A Weaver 4/30/82
8-30-82	Revised Draft for Review	Thomas K. Kipp 8/30/82	D A Weaver 8/30/82
11-11-82	Draft for Approval	Thomas K. Kipp 11/11/82	D A Weaver 11/11/82
2-10-82	Initial Issue	Thomas K. Kipp 2/10/83	D A Weaver 2/10/83

SEISMIC MARGIN REVIEW

MIDLAND ENERGY CENTER PROJECT

TABLE OF CONTENTS

TABLE OF CONTENTS

TABLE OF CONTENTS (Continued)

LIST OF TABLES

LIST OF FIGURES

LIST OF SYMBOLS

$\overline{A}$	=	section shear area
a,b,c,f,g,h,R_H	=	bolt chair dimensions
a_o	=	dimensionless frequency for soil-structure response
B	=	elastic buckling factor
C_H	=	horizontal soil-structure interaction impedance function damping constant
C_L	=	collapse load capacity
CM	=	code margin
C_ψ	=	rocking soil-structure interaction impedance function dashpot constant
C_v	=	vertical soil-structure interaction impedance function dashpot constant
D	=	tank diameter
d	=	maximum fluid slosh height
$d_H(a_o)$	=	horizontal frequency-dependent coefficient for soil damping
DL	=	dead load
$d_\psi(a_o)$	=	rocking frequency-dependent coefficient for soil damping
$d_v(a_o)$	=	vertical frequency-dependent coefficient for soil damping
E	=	modulus of elasticity
e	=	eccentricity of bolt chair load
F	=	hydrostatic pressure from ground water loading
f	=	frequency of the soil-structure mode
F_B	=	maximum anchor bolt force
f'_c	=	concrete unconfined compression strength
F.S.	=	factor of safety
F_{SME}	=	seismic margin
F_v	=	vertical seismic-induced forces on ring foundation
f_v	=	cyclic vertical natural frequency

LIST OF SYMBOLS (Continued)

g	=	gravity acceleration
G_e	=	effective shear modulus at seismic shear strains
$\check{G}_e$	=	median effective shear modulus
G_m	=	free-field small strain shear modulus
$\check{G}_m$	=	median free-field small strain shear modulus
G_{m_s}	=	small strain shear modulus including tank surcharge effect
H	=	lateral earth pressure loading
h	=	height of fluid in the tank
I	=	section moment of inertia
I_ψ	=	mass moment of inertia of the tank about its base
K_H	=	horizontal soil-structure interaction impedance function stiffness
K_ψ	=	rocking soil-structure interaction impedance function stiffness
K_v	=	vertical soil-structure interaction impedance function stiffness
$[K_e]$	=	element stiffness matrix
$[K_s]$	=	structure stiffness matrix
L	=	live load
$\ell, \alpha, \beta, R_{eff}$	=	bolt chair yield line dimensions
ℓ_t	=	portion of tank circumference tributary to each anchor bolt
M	=	seismic-induced overturning moment
$M_{①}, M_{②}, M_{③}, M_{④}$	=	hinge plastic moment capacities
M_2	=	seismic-induced overturning moment due to sloshing
M_B	=	seismic-induced overturning moment on tank bottom
M_I	=	mass of tank and impulsive water
M_{tw}	=	total mass of tank and water

LIST OF SYMBOLS (Continued)

OBE	=	Operating Basis Earthquake
P	=	anchor bolt load
p	=	pressure
P_1	=	hydrodynamic pressure on tank shell from the horizontal impulsive fluid mode
P_2	=	hydrodynamic pressure on tank shell from the horizontal sloshing fluid mode
P_{CAP}	=	bolt chair code capacity
P_{static}	=	hydrostatic pressure on the tank shell
$P_{vertical}$	=	hydrodynamic pressure on the tank shell due to vertical seismic response
R	=	tank radius
S	=	allowable stress intensity
Sa_1	=	spectral acceleration of the predominant horizontal impulsive mode
Sa_2	=	spectral acceleration of the sloshing mode
Sa_v	=	spectral acceleration for the vertical response mode
$s_H(a_o)$	=	horizontal frequency-dependent coefficient for soil stiffness
SME	=	Seismic Margin Earthquake
$s_\psi(a_o)$	=	rocking frequency-dependent coefficient for soil stiffness
$s_v(a_o)$	=	vertical frequency-dependent coefficient for soil stiffness
S_y	=	minimum specified yield strength
T	=	differential settlement loading
t	=	shell thickness
T_a	=	anchor bolt tension
U	=	code ultimate response from combination of all loads

LIST OF SYMBOLS (Continued)

V	=	seismic-induced base shear from tank and impulsive fluid response
V_s	=	soil shear wave velocity
V_2	=	seismic-induced base shear due to sloshing
W	=	total fluid weight
W_2	=	fluid effective sloshing weight
W_I	=	impulsive fluid weights
$w_I(y)$	=	impulsive weight per unit height
W_R	=	roof weight
W_S	=	shell wall weights
W_T	=	tributary weight of water directly above ring foundation
W_V	=	tank shell and fluid weight
X_2	=	height above tank base of W_2
y	=	depth of fluid measured from fluid surface
β_e	=	logarithmic standard deviation of G_e
β_m	=	logarithmic standard deviation for G_m
β_r	=	logarithmic standard deviation of (G_e/G_m)
γ	=	weight density
Δ	=	displacement
λ_e	=	element damping value
λ_H	=	fraction of critical damping for horizontal impulsive response
λ_m	=	fraction of critical damping for mth mode
λ_ψ	=	fraction of critical damping for rocking response

LIST OF SYMBOLS (Continued)

λ_s	=	soil material damping
λ_v	=	fraction of critical damping for vertical response
$[\lambda K_s]$	=	modified structure stiffness formed by multiplying element stiffness matrix by element damping
ν	=	Poisson's ratio
ξ	=	seismic shear strain
σ	=	bolt chair top plate stress or tank shell hoop stress
σ_{cr}	=	allowable buckling stress
σ_{DL}	=	compressive stress in tank shell due to dead load
$\sigma_{\ell m}$	=	local membrane hoop stress
σ_{ms}	=	tensile stress in tank shell due to seismic overturning moment
σ_o	=	free-field mean effective soil stress
σ_s	=	mean effective soil stress with surcharge
σ_T	=	tensile stress in the tank shell
σ_v	=	tensile stress in tank shell due to vertical earthquake
ϕ	=	concrete capacity reduction factor or soil angle of internal friction
$\{\phi\}_m$	=	mth mode eigenvector
ω_2	=	sloshing natural frequency
ω_v	=	vertical natural frequency

1. INTRODUCTION

1.1 PURPOSE AND SCOPE OF WORK

An evaluation of the borated water storage tanks (BWST) and their foundations for the Midland Nuclear Power Plant subjected to a Seismic Margin Earthquake (SME) and other loadings has been performed and is described herein. In this evaluation, site specific response spectra (SSRS) representative of the seismicity and soil conditions at the tank site have been used for the earthquake excitation. An envelope of the SSRS and the broad frequency content Housner response spectrum constitute the SME.

The Midland BWST's and their foundations have been evaluated based upon response spectrum seismic analysis. The tank has been represented by a lumped mass-beam element mathematical model with concentrated springs and dashpots for incorporating soil-structure interaction impedance functions. From the resulting seismic loads, the expected behavior of the tank shell, roof, ring wall and ring beam foundation and the underlying supporting soil has been evaluated.

The purpose of this evaluation is to demonstrate that an acceptable margin against failure or damage to the Midland BWST's when subjected to SME ground motion exists in the as-designed configuration. From the tank SME response combined with response from other loadings, the margin of safety relative to code allowable structural capacities has been assessed. This value is defined as the "code margin", CM. In addition, the factor by which the SME would have to increase (with other loadings held constant) in order to reach code allowable structural capacities has been evaluated. This value is defined as the "seismic margin", F_{SME}. For the evaluation of CM and F_{SME}, allowable code capacities are taken from the governing codes used for the design of the tanks and their foundations (see Chapter 4).

1.2 DESCRIPTION OF THE TANKS AND FOUNDATIONS

There are two BWST's in the Midland Nuclear Power Plant complex, one each for Units 1 and 2. Each BWST is a right vertical, circular cylindrical, flat-bottom tank with a diameter of 52 feet and a cylindrical wall height of 32 feet and an umbrella-shaped roof as shown in Figure VI-1-1. The tank wall is 3/8 inch thick for the bottom 8 feet and 1/4 inch thick for the remainder of the cylindrical shell height. The bottom plate is 1/4 inch thick. The tank roof is 0.3 inch thick with a 52 foot radius and a height of 6 feet, 9-3/8 inches. Tank material is Type 304L stainless steel. Borated water is stored in the tank up to a height of 32 feet.

The BWST's are located outdoors in the tank farm area, north of the Auxiliary Building. The Unit 1 tank, 1T-60, is located on the west side of the tank farm and the Unit 2 tank, 2T-60, is located on the east side of the tank farm. Tank details are shown on Graver drawings NL12046, Rev. 3, NL-12047, Rev. 2, and NL-12051, Rev. 2.

The tank shell, roof, and part of the water in the tank (above the foundation ring wall) are supported by a reinforced concrete ring foundation. Compacted granular fill lies inside the ring wall and a 6-inch layer of oiled sand is between the tank bottom and the granular fill. Approximately 25 feet of compacted plant fill lies under the foundation structure and granular fill. The tank shell is anchored to the reinforced concrete ring foundation by forty 1-1/2-inch diameter, 3 feet 6 inches long A36 anchor bolts. These anchor bolts, which are evenly spaced and embedded around the circumference of the ring wall, provide anchorage to the tank to resist overturning caused by seismic induced lateral load. Details of the anchor bolt and its connection (anchor bolt chair) to the tank shell are illustrated in Figure VI-1-2. The eccentricity of the anchor bolts relative to the outside of the tank wall have a nominal value of 3-inches. However, this dimension is not tightly controlled. Based upon field measurements of several bolt chairs, this dimension is considered to vary by $\pm$ 1/4-inch. Thus, the maximum eccentricity used in all calculations was 3.25 inches.

Ring walls for the two tanks are identical except in the valve pit area. Unit 1 has a larger valve pit than Unit 2. The reinforced concrete ring foundation which supports the tank shell and some of the stored water, consists of an originally constructed ring wall (1 foot 6 inches wide by 4 feet 6 inches high) and its footing (4 feet wide by 1 foot 6 inches high) and a ring beam (2 feet wide by 4 feet 6 inches high) integrally tied to the original ring wall. The ring beam was added as a result of the remedial soils program for this plant. Shear connectors which are installed to the original ring wall by drilling and grouting at one end and cast in the ring beam at the other end, are used to integrally tie the ring wall and the ring beam together. Figure VI-1-3 gives the cross-section detail of the ring foundation. The minimum specified concrete compressive strength (f'_c) is 4000 psi. Grade 60 reinforcement is assumed to be used in the foundation construction. The outer radius of this ring foundation is 28.75 feet. The inner radius is 24 feet. These values are utilized in the calculation of soil-spring and dashpot constants.

1.3 SEISMIC GROUND MOTION

The earthquake excitation for the Midland Seismic Margin Evaluation program is specified in terms of ground response spectra. This response spectra is the envelope of the SSRS developed by Weston Geophysical Corporation (Reference 1) for structures founded at the top-of-fill and the Housner response spectra (Reference 2) which is anchored to a 0.12g zero period (peak) ground acceleration. The individual SSRS and Housner spectra are illustrated in Figure VI-1-4 for 20 percent of critical damping. The envelope spectrum for horizontal ground motion is illustrated in Figure VI-1-5 for various damping levels. The vertical ground motion component is defined as 2/3 of the enveloped horizontal motion illustrated in Figure VI-1-5. Peak (zero period) horizontal ground acceleration at plant grade elevation is about 0.15g.

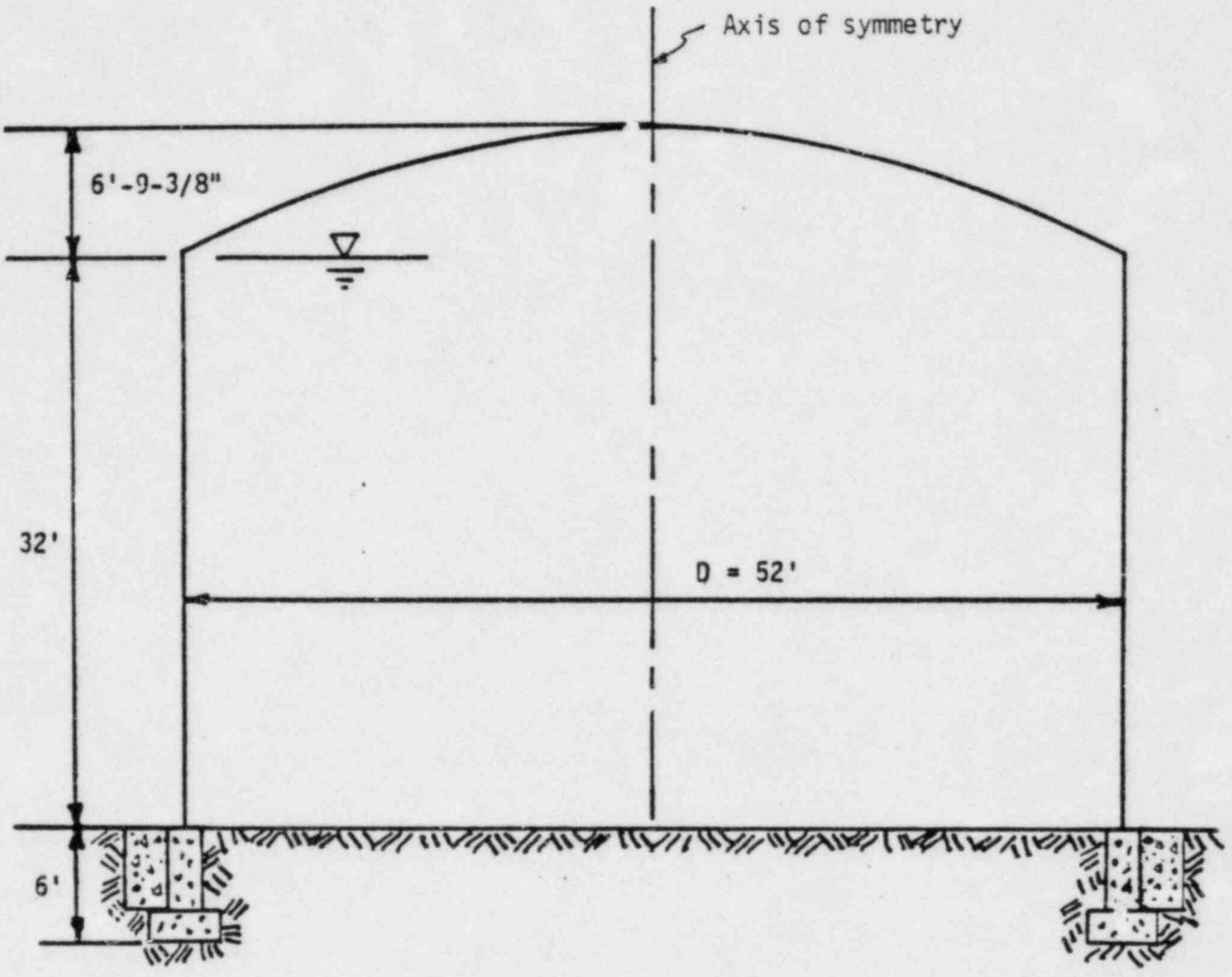

FIGURE VI-1-1. BORATED WATER STORAGE TANK CONFIGURATION

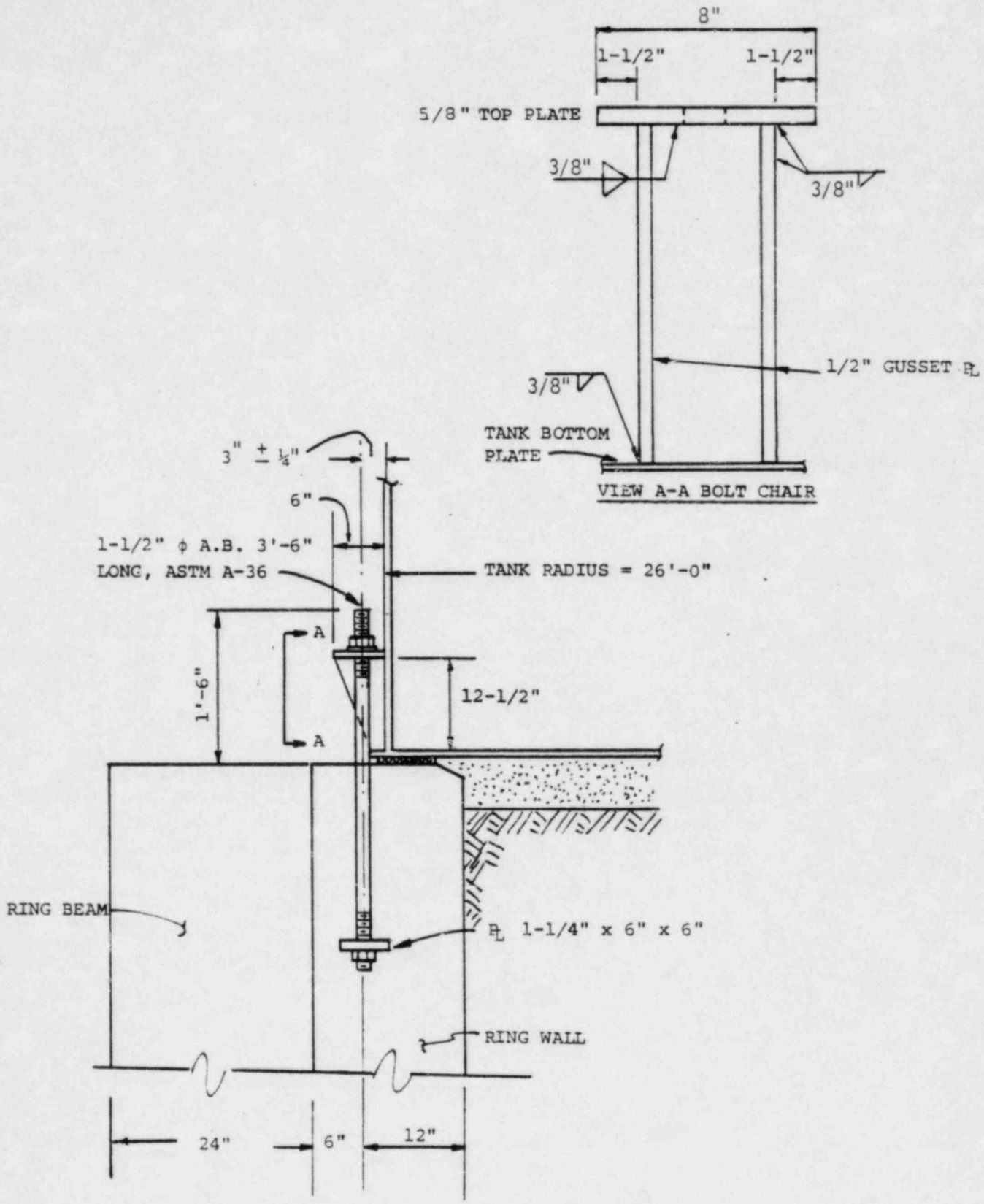

FIGURE VI-1-2. BWST ANCHOR BOLT AND BOLT CHAIR DETAIL

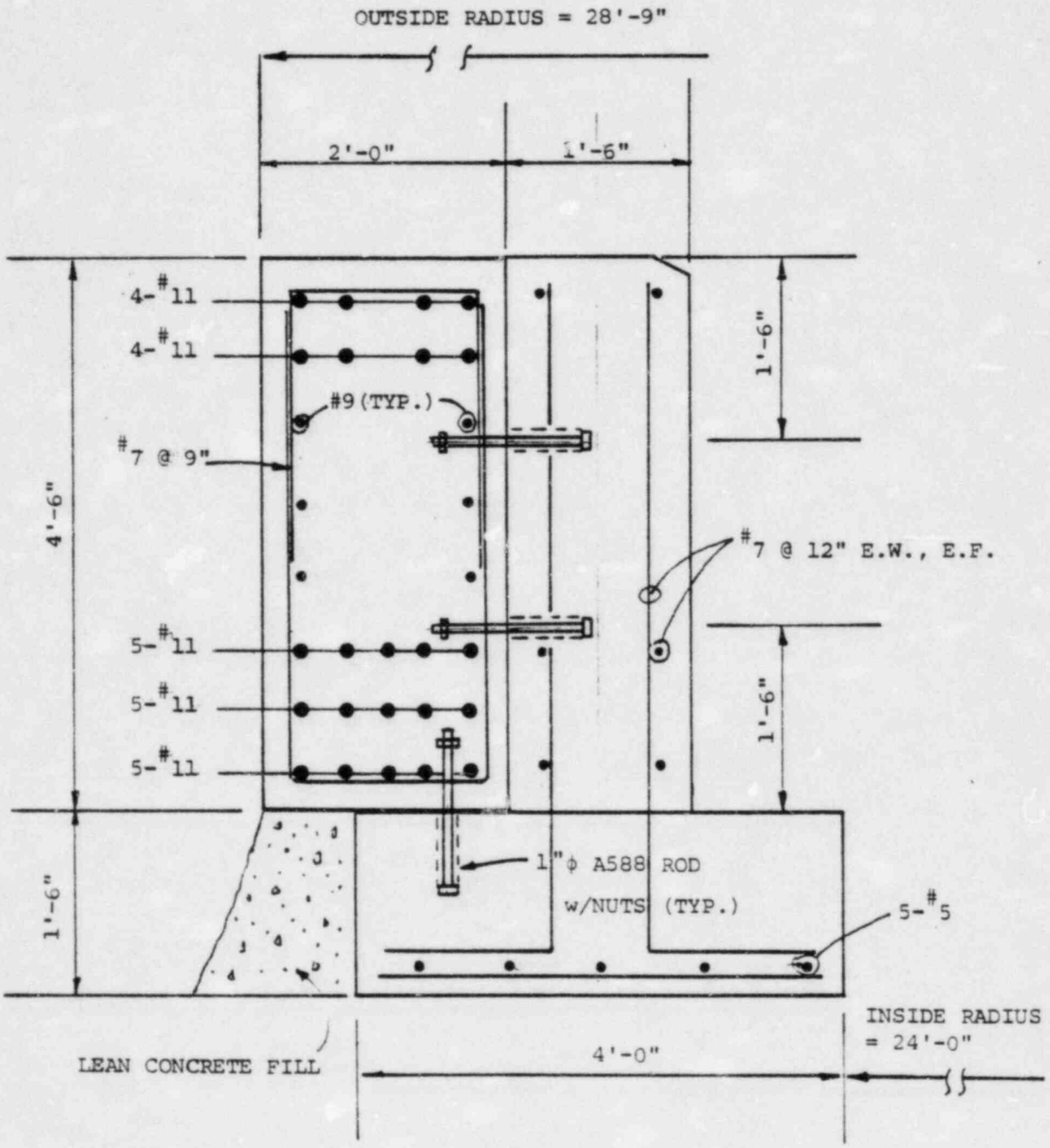

FIGURE VI-1-3. BWST CONCRETE RING FOUNDATION DETAIL

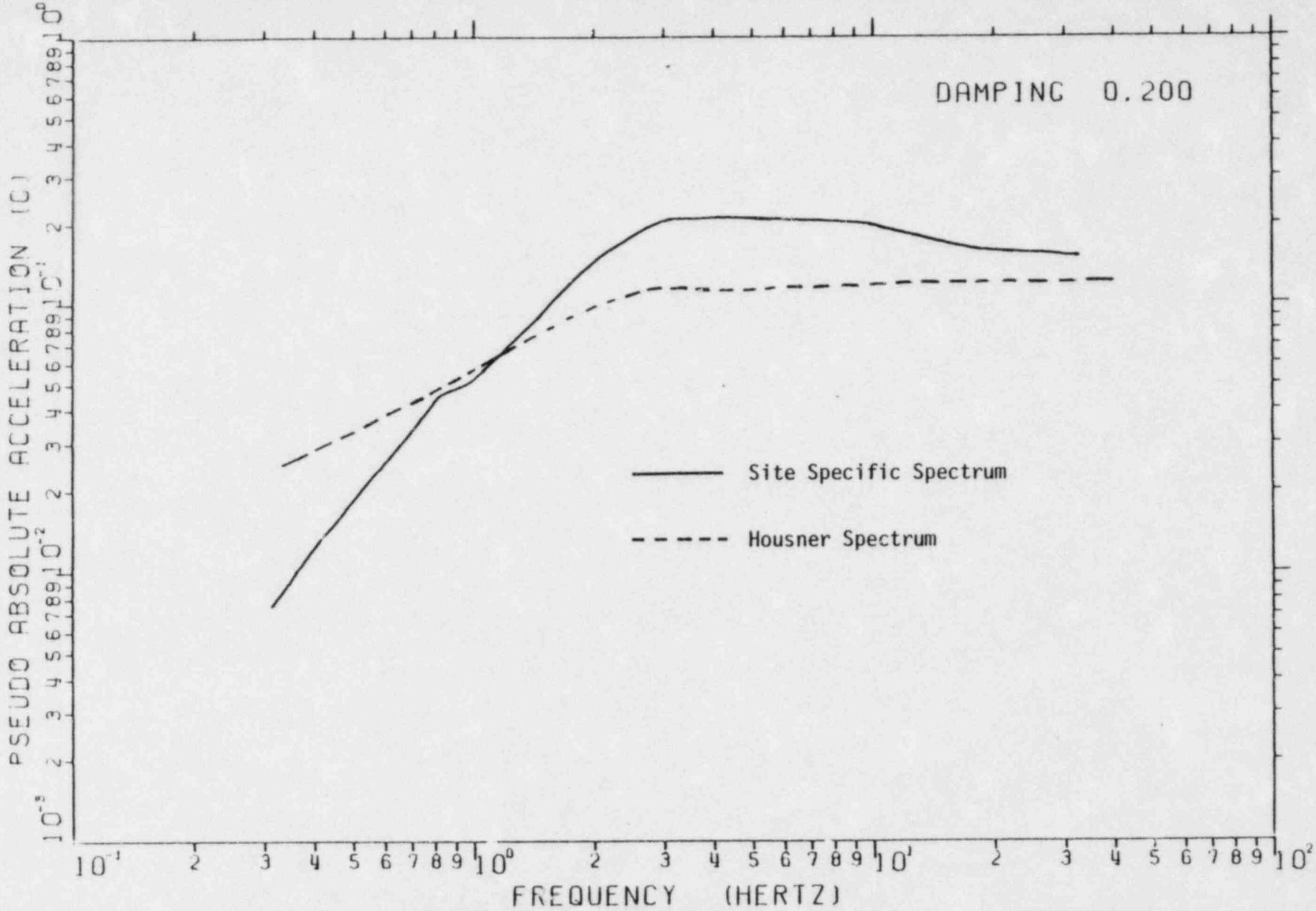

MIDLAND - HOUSNER SPECTRUM

VI-1-4. MIDLAND - TOP OF FILL SITE SPECIFIC SPECTRUM AND HOUSNER SPECTRUM (20 Percent of Critical Damping)

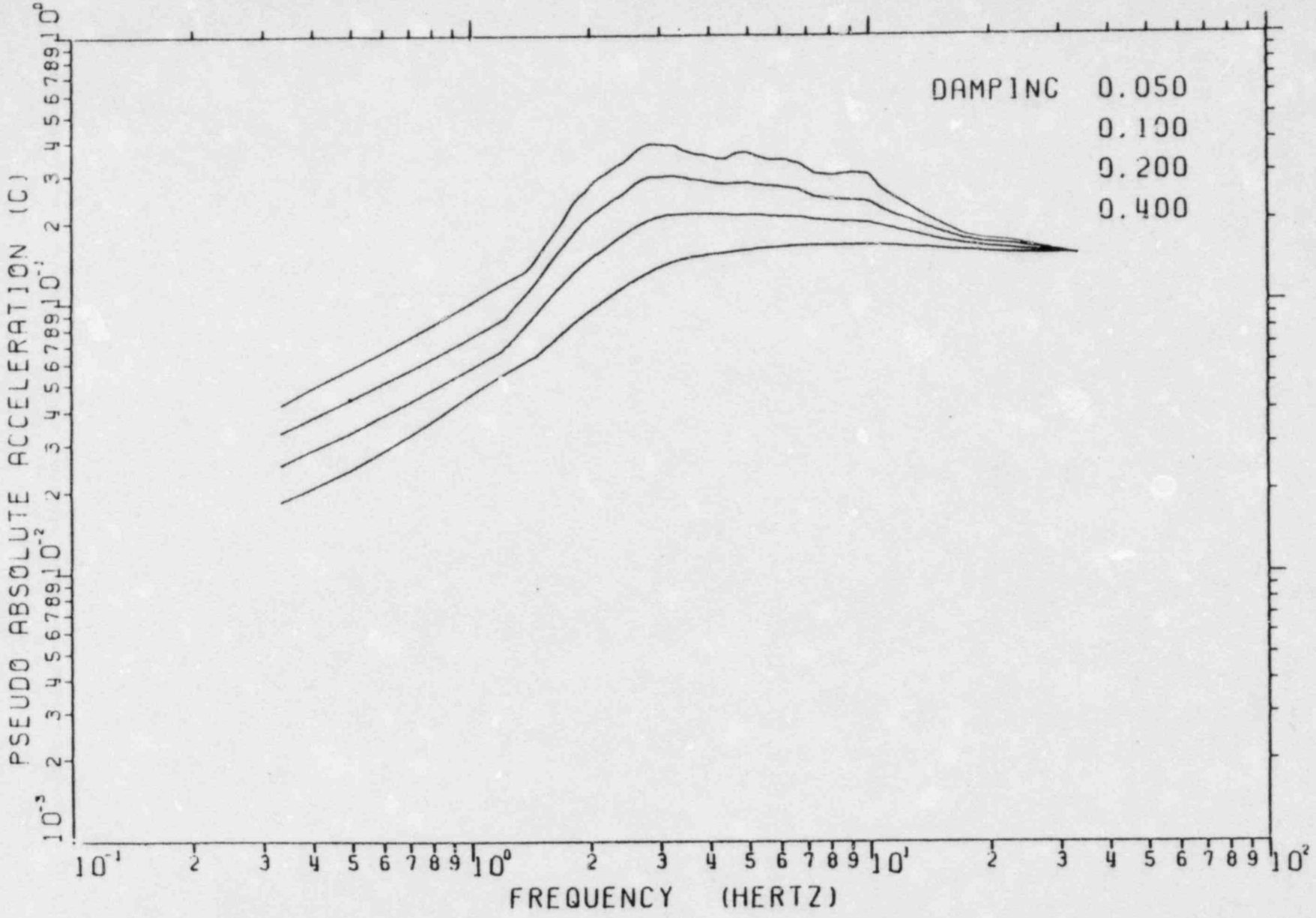

FIGURE VI-1-5. MIDLAND - SEISMIC MARGIN EARTHQUAKE (SME) TOP OF FILL ENVELOPE RESPONSE SPECTRA

2. SEISMIC ANALYSIS METHOD

2.1 GENERAL

The general analytical approach used to evaluate the BWST is outlined in the following paragraphs and detailed descriptions of the seismic model and treatment of soil-structure interaction and damping are addressed in subsequent sections.

The tank shell weight is supported on the concrete foundation which must also withstand the seismic-induced forces in the tank shell. The seismic forces in the tank shell are nearly totally due to the water in the tank. The tank shell weight is negligible compared to the weight of the water. Thus, the primary seismic modeling concern is to conservatively model the seismic forces induced by this water on the tank shell and thus, on the foundation. The seismic-induced effects of the water on the BWST can be considered in three parts; 1) the impulsive mode; 2) the sloshing mode; and 3) the vertical mode of fluid-structure interaction. Each of these modes of response is best modeled with its own individual model. The seismic forces imposed upon the tank shell and foundation from each of these three models are combined by the square-root-sum-of-squares (SRSS) method.

Soil-structure interaction has been incorporated into the analysis by use of frequency-dependent impedance functions. The soil beneath the tank was treated as an elastic half-space corrected to account for minor layering effects of the soil beneath the BWST. Best estimated soil properties have been evaluated from test data on the underlying fill and till material to establish impedance function "spring stiffnesses" and "dashpot constant" values. Strain degradation of the soil stiffness properties (approximate nonlinear behavior of the soil) was accounted for in establishing the impedance functions. To account for uncertainties in soil properties and in the mathematical modeling of

soil-structure interaction, the soil-structure interaction stiffnesses are varied within the range from 0.6 to 1.67 times the "best estimate" soil-structure interaction stiffnesses. The seismic-induced loads are based on the envelope of seismic responses obtained for soil-structure interaction stiffnesses which vary throughout this range of possible stiffnesses.

Energy dissipation within the tank, fluid and soil system is approximated in the dynamic models as viscous (velocity proportional) damping. Damping consists of material (hysteretic) damping and radiation damping or the radiation of energy from the structure back into the supporting soil. In order to conservatively account for effects of soil layering or variation of properties with depth, the soil radiation damping used in the seismic evaluation have been taken as 75 percent of the theoretical elastic half-space values.

2.2 SEISMIC MODEL

2.2.1 IMPULSIVE MODE

The dynamic model of the BWST used for determining the seismic forces on the ring foundation from the horizontal impulsive fluid mode is illustrated schematically in Figure VI-2-1. The tank shell stiffness is modeled by vertical beam elements between mass points distributed up the tank shell. The beam elements represent the shear and flexural stiffness of the tank. The ovalling stiffness of this tank is judged to be insignificant to the seismic response as the tank is held in round by its base at the bottom and by the roof at the top. The roof weight, W_R, is lumped at the roof level. The shell wall weights, W_S, are lumped at discrete points on the tank shell. Impulsive fluid effective weights, W_I, are added to the tank shell weights at each of these node points at and below the top surface of the fluid. For computations of tank seismic response, a rigid link between impulsive fluid weights and shell wall weights as is schematically shown on Figure VI-2-1 is not required. The actual model used for evaluating horizontal impulsive seismic response is illustrated in Figure VI-2-2. Numerical values for the weights, tank stiffness and geometry are presented on this figure.

For a rigid mode of horizontal tank vibration, it has been shown by Housner (Reference 2) that the total effective horizontal impulsive weight of the fluid, W_I is given by:

$$W_I = \frac{W \tanh(0.866\ D/h)}{0.866\ D/h} \qquad (2\text{-}1)$$

where W = total fluid weight
D = tank diameter
h = fluid height

This total effective impulsive weight is distributed parabolically over the fluid height as shown in Figure VI-2-1. The impulsive weight per unit height, $w_I(y)$, over the fluid height is given by:

$$w_I(y) = 0.866\ \pi\gamma Dh \left[\tanh(0.866\ D/h)\right]\left[\frac{y}{h} - \frac{1}{2}\left(\frac{y}{h}\right)^2\right] \qquad (2\text{-}2)$$

where γ = fluid density
y = is the depth of fluid measured from the fluid surface

With a flexible tank, the impulsive fluid effects should more precisely be considered as an impulsive pressure rather than effective impulsive weights. However, it has been shown by Veletsos (Reference 6) that the effective impulsive weight distribution developed by Housner for rigid tanks can be used to conservatively predict impulsive mode base shears and overturning moments at the bottom of flexible tanks (i.e., the forces on the ring foundation). For tanks similar to the BWST, this approximation leads to base shears which are between a factor of 1.1 and 1.2 times greater than would be obtained using flexible tank impulsive pressures. The overturning moments obtained assuming a Housner effective weight distribution are within 2 percent of those obtained using a flexible tank impulsive pressure distribution. This slight improvement in accuracy does not warrant the substantial added effort of treating the tank shell as flexible when determining the impulsive fluid effects. The

effective impulsive fluid weight distribution given by Equation 2-2 and shown in Figure VI-2-1, is adequate for computing seismic-induced base shear and overturning moment for the impulsive mode.

Note that for evaluating hoop streses in the shell wall of flexible tanks, a more accurate representation of hydrodynamic pressures over the tank height is needed as the pressure distribution derived for a rigid wall tank (Equation 2-2) is unconservative for the upper portion of the tank and overly conservative near the base of the tank. For computation of tank wall stresses, the hydrodynamic pressure, P_1, on the tank shell resulting from the horizontal impulsive fluid mode at depths y from the top of the fluid greater than 0.15h have been obtained from:

for $y/h \geq 0.15$

$$P_1 = \frac{V}{1.453\ Dh} \qquad (2\text{-}3)$$

where V = the seismic-induced base shear as determined from the response spectrum seismic analysis.

The pressure increases linearly from the top of the fluid (y = 0) to the value from Equation 2-3 at y = 0.15h and greater. Equation 2-3 provides an adequate description of the pressure distribution with respect to height on the tank shell for a flexible tank which is in reasonable agreement with the results presented in References 6 and 7 for flexible tanks.

The seismic model shown in Figure VI-2-2 is suitable for computing seismic-induced loads on the concrete foundation for the horizontal impulsive mode. There are also seismic-induced loads on the tank bottom. These loads may be expressed as an additional overturning moment applied over the area of the tank bottom. The additional overturning moment, M_B can be conservatively evaluated by the following expression taken from Reference 2:

$$M_B = 0.1045\ DWSa_1 \qquad (2\text{-}4)$$

where Sa_1 = is the spectral acceleration of the predominant horizontal impulsive mode

For the BWST, this moment is applied primarily to the soil inside the ring wall foundation and not to the concrete foundation directly. However, this moment does result in some additional forces on the foundation due to the effect of the water directly above the concrete foundation.

2.2.2 SLOSHING MODE

The horizontal fluid sloshing mode is a long period (low-frequency) mode of vibration. Because of its low frequency, this mode of vibration does not interact with the effects of tank flexibility or soil-structure interaction. A dynamic model is not required in order to evaluate the forces imposed on the tank shell and ring foundation by this mode. The natural frequency of vibration, ω_2, of this mode, the fluid effective sloshing weight, W_2, and height of application, X_2, above the tank base are given by relations from References 2 and 7 as presented below.

$$\omega_2^2 = \frac{3.67g}{D} \tanh\left(\frac{3.67h}{D}\right) \qquad (2\text{-}5)$$

$$W_2 = 0.230\ \frac{WD}{h} \tanh\left(\frac{3.67h}{D}\right) \qquad (2\text{-}6)$$

$$X_2 = h - \frac{h\cosh\left(\frac{3.67h}{D}\right) - h}{\frac{3.67h}{D}\sinh\left(\frac{3.67h}{D}\right)} \qquad (2\text{-}7)$$

where g = gravity acceleration (32.17 ft/second^2).

The base and overturning moment at the tank shell base due to this sloshing mode are given by:

$$V_2 = W_2 Sa_2 \tag{2-8}$$

$$M_2 = W_2 X_2 Sa_2 \tag{2-9}$$

where Sa_2 = the spectral acceleration at frequency ω_2.

To evaluate tank shell stresses, the hydrodynamic pressure, P_2, on the tank shell resulting from the horizontal sloshing fluid mode at depth y from the top of the fluid has been evaluated by:

$$P_2 = \frac{0.533\ WSa_2}{Dh} \frac{\cosh\left(3.68\ \frac{h-y}{D}\right)}{\cosh\left(3.68\ h/D\right)} \tag{2-10}$$

To evaluate the potential effects of sloshing on the tank roof, the fluid slosh height, d, has been estimated from:

$$d = 0.42\ DSa_2 \tag{2-11}$$

2.2.3 VERTICAL MODE

In the vertical mode, the water in the tank is supported directly on the soil and the tank itself is very stiff. Therefore, both the tank and the fluid can be modeled as rigid in this mode. The only source of flexibility comes about because of soil-structure interaction effects. A dynamic model is not required for such a simple problem. The natural frequency of vibration is given by:

$$\omega_v = \sqrt{\frac{K_v g}{W_v}} \tag{2-12}$$

where W_v is the sum of the tank shell weight, W_s, and the total fluid weight, W, and K_v is the vertical soil-structure interaction impedance function stiffness. This is a rigid structure mode of vibration for which the fraction of critical damping, λ_v, is given by:

$$\lambda_v = \frac{0.75\ C_v}{2\sqrt{K_v W_v/g}} + \lambda_s \qquad (2\text{-}13)$$

where C_v is the vertical dashpot coefficient from the soil-structure interaction impedance function for the foundation, g is gravity acceleration (32.17 feet/second^2), and λ_s is the appropriate soil material damping (5 percent of critical as discussed in Section 2.4.1). The 0.75 factor is included to account for soil layering effects as discussed in Section 2.1

The ring wall foundation primarily supports the vertical seismic forces from the shell. The vertical fluid forces are supported directly on the soil. However, it should be noted that the tributary weight of water located directly above the ring wall, W_T, does result in additional vertical seismic loads on the foundation. Thus, the vertical seismic forces on the ring foundation are given by:

$$F_v = Sa_v(W_s+W_T) \qquad (2\text{-}14)$$

where Sa_v represents the design seismic vertical spectral acceleration at damping level, λ_v, and cyclic natural frequency, f_v, where $f_v = \omega_v/2\pi$.

2.3 SOIL-STRUCTURE INTERACTION

2.3.1 Soil Properties

The soil profile beneath the BWST has been estimated based upon several sources. The fill properties extend from elevation 610 to 634. The original glacial till extends down from elevation 610 to elevation 410. A very dense, granular soil extends from elevation 410 to bedrock at elevation 520. The fill properties were based upon estimates made by Dr. Woods (Reference 8) and Weston Geophysical (Reference 1). The original till properties were based upon estimates from Weston Geophysical (Reference 1) and Dames & Moore (Reference 10). Based upon these references, the soil profile presented in Figure VI-2-3 was developed. This figure shows the most probable range for density, γ, Poisson's ratio, ν, shear wave velocity, V_s, and free-field small strain shear modulus, G_m, for each layer beneath the BWST down to elevation 463. Properties beneath elevation 520 could not possibly influence the soil-structure interaction properties for the BWST. Thus, this profile was not extended below elevation 463. Figure VI-2-3 shows that shear wave velocity and free-field small strain shear modulus increase with depth. Although Figure VI-2-3 divides the soil profile into several layers, the actual increase in stiffness is considered to be gradual rather than in abrupt layers down to elevation 553 where an abrupt layer change is likely to exist. The soil profile between elevation 628 (bottom of ring foundation) and elevation 571 primarily influences the soil-structure interaction properties for the BWST. Based upon a weighted averaging of the soil properties between elevation 571 and 628, it was estimated that the average free-field small strain shear modulus value has the following median and logarithmic standard deviation values:

$$G_m \approx 2.4 \times 10^3 \text{ ksf}$$
$$\beta_m \approx 0.19 \qquad (2\text{-}15)$$

which corresponds to a plus and minus one standard deviation range of

$$G_m = 2.0 \text{ to } 2.9 \times 10^3 \text{ ksf}$$

Several corrections must be applied to the average free-field small strain shear modulus before it can be used to estimate soil-structure interaction effects. First, the tank and fluid weight apply a surcharge to the upper layers of soil in the immediate vicinity of the tank and this surcharge effectively increases the small strain shear moduli for these upper layers. Secondly, for the SME, the seismic strains associated with these soft upper layers are not small and the effective shear moduli of these upper layers must be reduced below the small strain shear moduli to account for the high seismic strain levels.

Based upon the Hardin and Drnevich approach (Reference 10), the tank surcharge effect on the small strain shear modulus can be estimated from

$$G_{m_s} \approx G_m \sqrt{\sigma_s/\sigma_o} \qquad (2\text{-}16)$$

where G_{m_s} is the small strain shear modulus corrected for surcharge, σ_s is the mean effective stress with surcharge and σ_o is the free-field mean effective stress. The following estimates of G_{m_s}/G_m have been made:

$$\begin{aligned} &\text{Elevation 625:} \quad G_{m_s}/G_m = 1.3 \text{ to } 1.6 \\ &\text{Elevation 595:} \quad G_{m_s}/G_m = 1.0 \text{ to } 1.2 \end{aligned} \qquad (2\text{-}17)$$

Estimates of intermediate elevations can be obtained by interpolation.

Figure VI-2-4 (from Reference 10) presents the relationship between the effective shear modulus at higher seismic shear strains, G_e, and the small strain shear modulus, G_{m_s}. The following ranges of seismic shear strains, γ, have been estimated for the seismic margin earthquake level:

Elevation 625: $\gamma = 0.08$ to 0.04%

Elevation 595: $\gamma = 0.04$ to 0.02% (2-18)

Based upon these estimates, the corresponding range of G_e/G_{m_s} from Figure VI-2-4 are:

Elevation 625: $G_e/G_{m_s} = 0.25$ to 0.45

Elevation 595: $G_e/G_{m_s} = 0.30$ to 0.60 (2-19)

Combining the results of Equation 2-17 and 2-19, it is estimated that throughout the profile from Elevation 628 to 571, the ratio of effective shear modulus to free-field small strain shear modulus has the following median and logarithmic standard deviation values:

$$(\overset{\vee}{G_e/G_m}) \approx 0.48$$

$$\beta_R \approx 0.46 \quad (2\text{-}20)$$

which corresponds to a plus and minus one standard deviation range of:

$$(G_e/G_m) = 0.30 \text{ to } 0.75$$

Combining Equations 2-15 and 2-20, the effective shear modulus has the following median and logarithmic standard deviation values:

$$\overset{\vee}{G}_e \approx 1.15 \times 10^3 \text{ ksf}$$

$$\beta_e \approx 0.50 \quad (2\text{-}21)$$

Thus, the corresponding plus and minus one standard deviation range is:

$$G_e = 0.69 \text{ to } 1.90 \times 10^3 \text{ ksf}$$

In determining soil-structure interaction parameters, the following three values for effective shear modulus were used:

	Low	Intermediate	High	
G_e (ksf) =	0.69×10^3	1.15×10^3	1.90×10^3	(2-22)

As will be subsequently shown, the low value of effective shear modulus (0.69×10^3 ksf) leads to the largest RWST seismic responses for the seismic margin earthquake.

The following effective values for Poisson's ratio, and soil density were used in evaluating soil-structure interaction properties;

Poisson's Ratio:	$\upsilon = 0.45$	(2-23)
Density:	$\gamma = 115$ pcf	

The lower bound density of 115 pcf was used in order to conservatively underestimate radiation damping effects of the soil.

2.3.2 Soil-Structure Interaction Impedance Functions

Soil-structure interaction impedances have been modeled by the usage of the lumped parameter stiffness approach. Thus, the resisting forces which are developed when the structure moves relative to the surrounding soil mass are incorporated into the analytical model by means of impedance functions represented as equivalent springs and dashpots connecting the structure to the ground.

The resisting forces developed when the structure moves relative to the underlying soil, which are applied at the soil-structure interface, are illustrated in Figure VI-2-5a. In Figure VI-2-5b, the equivalent soil springs by which the resisting forces at the soil-structure interface are included in the structural model are illustrated. Note that there are horizontal and vertical translational springs and a rotational

spring to include forces at the interface of the soil and the bottom of the foundation. The forces and moments at the soil-structure interface are developed during seismic response of the structure.

In addition to the soil springs shown in Figure VI-2-5b, corresponding soil dashpots are included to incorporate the damping of the soil in the soil-structure model. Soil damping is composed of two types of damping: one introduced by the loss of energy through propagation of elastic waves from the immediate vicinity of the foundation (i.e., feedback of energy from the structure to the surrounding soil), and the other being material or internal damping associated with energy losses within the soil due to hysteretic or viscous effects. Material damping for the soil underlying the Midland 3WST is assumed to be 5 percent of critical damping (see Section 2.4.1). The calculation of dashpot constants to represent energy feedback is described below. Energy feedback is often called geometrical or radiation damping.

Values for soil springs and dashpots have been calculated based on formulas from References 4 and 5. These formulas are approximate analytical solutions for the condition of a rigid structure resting on an elastic half-space. Soil spring (K_H, K_v and K_ψ) and dashpot (C_H, C_v and C_ψ) constants for horizontal and vertical translational motion and for rocking motion are determined from the following relations:

Horizontal Translation

$$K_H = s_{H(a_o)} \frac{8G_eR}{(2-\nu)} \tag{2-24}$$

$$C_H = d_{H(a_o)} \frac{8G_eR^2}{(2-\nu)} \sqrt{\gamma/G_e g} \tag{2-25}$$

$$\lambda_H = \frac{0.75\ C_H}{2\sqrt{K_H M_I}} + \lambda_s \tag{2-26}$$

Rocking

$$K_\psi = s_\psi(a_o) \frac{8G_eR^3}{3(1-\nu)} \tag{2-27}$$

$$C_\psi = d_\psi(a_o) \frac{8G_eR^4}{3(1-\nu)} \sqrt{\gamma/G_e g} \tag{2-28}$$

$$\lambda_\psi = \frac{0.75\, C_\psi}{2\sqrt{K_\psi I_\psi}} + \lambda_s \tag{2-29}$$

Vertical Translation

$$K_v = s_v(a_o) \frac{4G_eR}{1-\nu} \tag{2-30}$$

$$C_v = d_v(a_o) \frac{4G_eR^2}{1-\nu} \sqrt{\gamma/G_e g} \tag{2-31}$$

$$\lambda_v = \frac{0.75\, C_v}{2\sqrt{K_v M_{tw}}} + \lambda_s \tag{2-32}$$

where R = the tank radius

M_{tw} = the total mass of tank and water

M_I = the mass of tank and impulsive water

I_ψ = the mass moment of inertia of the tank about its base

λ_H, λ_ψ and λ_v = radiation damping plus soil material damping in the horizontal, rocking and vertical directions expressed as fractions of critical damping

$S_H(a_o)$, $d_H(a_o)$, $s_\psi(a_o)$, $d_\psi(a_o)$, $s_v(a_o)$, $d_v(a_o)$ = coefficients which are dependent on the dimensionless frequency parameter a_o as shown in Figure VI-2-6.

$a_o = 2\pi f R \sqrt{\gamma/G_e g}$

f = the frequency of the seismic response for the soil-structure mode.

g = gravity acceleration

For horizontal and vertical translation, seismic-induced forces are transmitted to the underlying soil over the entire tank and ring wall area. Thus, the tank radius used in Equations 2-24, 2-25, 2-30 and 2-31 for horizontal and vertical translation is 28.75 feet to the outside of the ring wall. However, in rocking, seismic-induced forces are transmitted to the underlying soil primarily through the ring wall foundation. Thus for the rocking stiffness and damping, the spring and dashpot constants were evaluated by utilizing Equations 2-27 and 2-28 with the outer foundation radius of 28.75 feet and then subtracting from the resulting values the stiffness and damping corresponding to these equations for the inner foundation radius of 24 feet.

The frequency-dependent coefficients (s_H, d_H, etc.) were determined from Figure VI-2-6 using a coupled horizontal translational and rocking natural frequency of 4.6 hz and a vertical mode natural frequency of 5.6 hz which will be subsequently shown to be the best estimate fundamental horizontal impulsive and vertical mode natural frequencies. The resultant frequency-dependent coefficients are:

		Frequency-Dependent Coefficient for Stiffness	Frequency-Dependent Coefficient for Damping
Horizontal Translation (R = 28.75 ft.)		0.96	0.59
Rocking	R = 28.75 ft.	0.72	0.19
	R = 24 ft.	0.77	0.16
Vertical Translation (R = 28.75 ft.)		0.69	0.86

To account for minor layering effects, the radiation damping portion of the values (λ_H, λ_ψ, and λ_V) given by Equations 2-25, 2-29 and 2-32 are taken as 75% of the theoretical elastic half-space values. Soil material damping of 5% of critical is added to the radiation damping.

The best estimate (G_e = 1.15 x 10^3 ksf) soil stiffness and radiation damping values are as follows:

	Horizontal Translation	Rocking	Vertical Translation
Stiffness, K_H, K_ψ, or K_V	1.629×10^5 kip/ft	3.598×10^7 $\frac{\text{ft-kip}}{\text{rad}}$	1.650×10^5 kip/ft
Radiation Damping C_H, C_ψ, or C_V	5125 $\frac{\text{k-sec}}{\text{ft}}$	7.536×10^5 k-sec-ft	10470 $\frac{\text{kip-sec}}{\text{ft}}$
Radiation Damping plus soil material damping λ_H, λ_ψ, or λ_V	0.56	0.39	0.88

To account for uncertainty in the effective soil modulus, the soil shear modulus was varied over the range of about 0.6 to 1.67 times the best estimate value as discussed previously. Variation in soil shear modulus linearly affects the soil stiffness and does not change the radiation damping expressed as fraction of critical damping. Note that frequency dependent effects are assumed to be covered by varying shear modulus and frequency dependent parameters are not recomputed for lower and upper bound soil cases.

2.4 DAMPING

2.4.1 Material Damping

Fluid Sloshing	0.5 percent of critical damping
Tank Shell and Impulsive Fluid	4.0 percent of critical damping
Soil Material	5.0 percent of critical damping

The tank shell and impulsive fluid value is consistent with damping values specified for the SSE in USNRC Reg. Guide 1.61 (Reference 3). Reference 19 demonstrates that 5 percent damping is conservative for either sand or clay soil conditions at shear strains of 0.01 percent or greater. In Reference 20, 0.5 percent of critical damping is recommended for the horizontal sloshing mode unless a higher value can be substantiated by experimental results.

2.4.2 Equivalent Modal Damping

The damping approach used for the evaluation of the Midland BWST is to compute equivalent modal damping by assuming that the element damping is proportional to the element stiffness for each element. Thus, for the mth mode, the equivalent modal damping value λ_m is given by:

$$\lambda_m = \frac{\{\phi\}_m^T [\lambda K_s]\{\phi\}_m}{\{\phi\}_m^T [K_s]\{\phi\}_m} \qquad (2\text{-}33)$$

where $\{\phi\}_m$ is the mth mode eigenvector, $[K_s]$ is the overall structural stiffness matrix, and $[\lambda K_s]$ is a modified structural stiffness matrix formed by multiplying each element stiffness matrix $[K_e]$ by the element damping value λ_e prior to adding the modified element stiffness matrix into the structural stiffness matrix.

For horizontal impulsive modes, which are a combination of structural response and soil-structure interaction, modal damping values are not permitted to exceed 20% of critical. This upper limit was established to provide conservative composite modal damping values. This limit was validated by comparing (best estimate soil conditions) the base shear and overturning moment from modal time history analyses in which a 20% damping cutoff is used with those from direct integration time history analyses in which concentrated dashpots with properties given in the preceding section are used to represent soil radiation damping. The modal analysis with a composite modal damping cutoff of 20% led to base shears and overturning moments equal to 1.14 and 1.06 times those obtained from time history anlaysis with concentrated soil dashpots. Thus, the use of a 20 percent cutoff for modal damping produces reasonable and conservative tank seismic response from analyses of the horizontal impulsive tank-fluid mode.

The horizontal fluid-sloshing mode was 0.5% damped. The vertical response mode consisted entirely of soil response with a rigid structure. The full vertical soil-structure interaction damping was assigned to this mode with no upper bound limit on modal damping because no questions exist on the accuracy of composite modal damping for this pure soil mode of response.

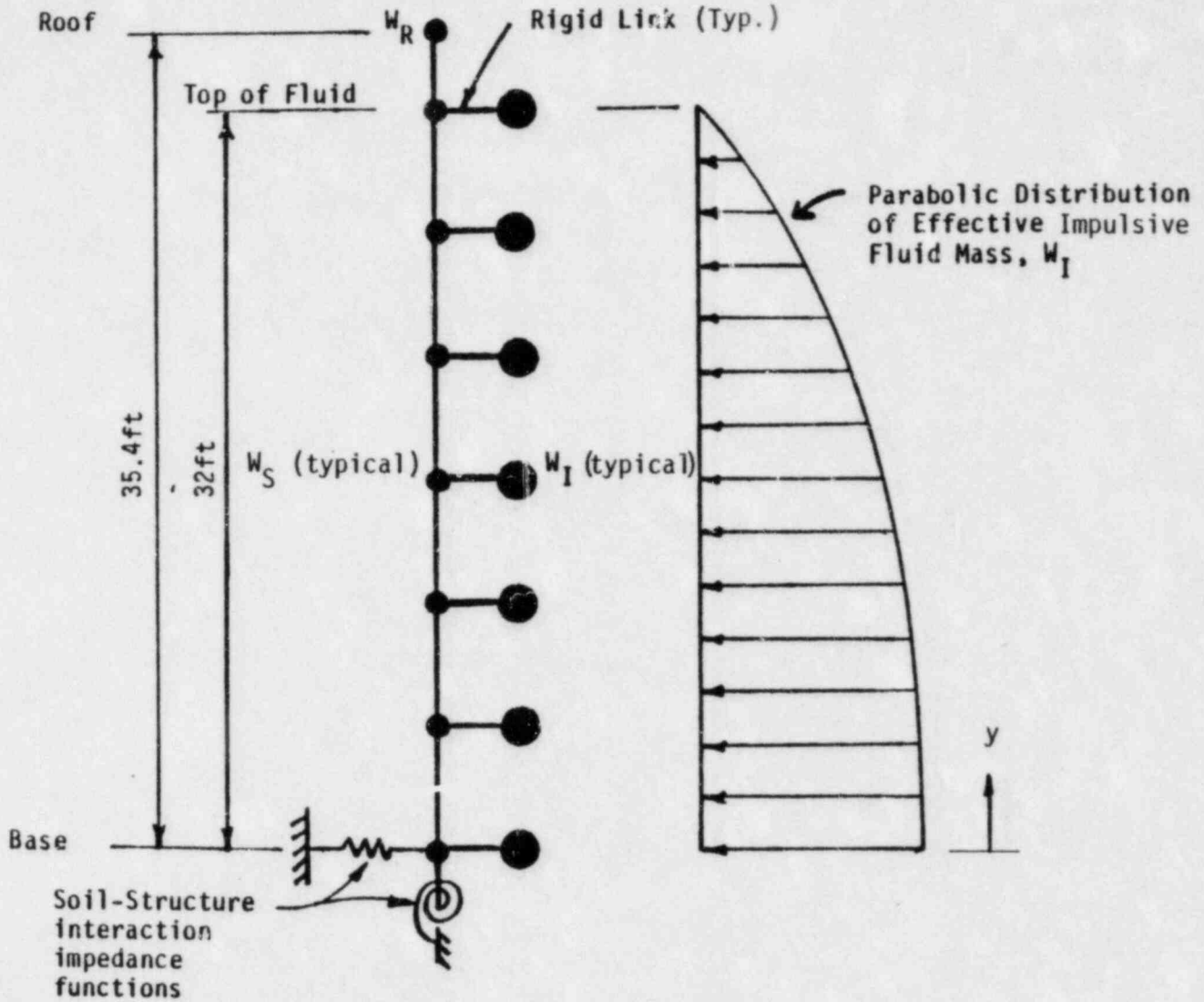

FIGURE VI-2-1. BWST HORIZONTAL IMPULSIVE MODE MODEL

TANK SHELL PROPERTIES

$E = 4.176 \times 10^6$ ksf; $\nu = 0.3$

t	$\bar{A}$	I
1/4"	1.70 ft^2	1150 ft^4
3/8"	.55 ft^2	1726 ft^4

$\bar{A}$ = Shear Area

I = Moment of Inertia

SOIL IMPEDANCE FUNCTION PROPERTIES

STIFFNESS

	K_H (k/ft)	K_ψ (k-ft/rad)
Lower Bound	0.977×10^5	2.159×10^7
Best Estimate	1.629×10^5	3.598×10^7
Upper Bound	2.72×10^5	6.009×10^7

DAMPING

$\lambda_H = 56\%$

$\lambda_\psi = 39\%$

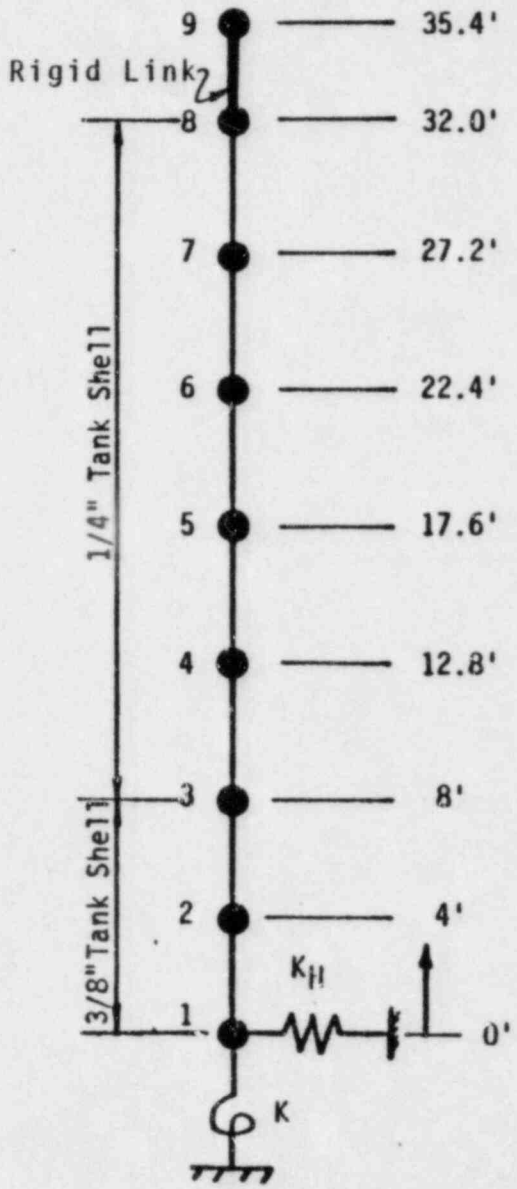

Node No.	Weight (kips)*
1	277.9
2	503.6
3	523.8
4	512.1
5	426.0
6	312.7
7	172.3
8	25.9
9	28.6

* $W_S + W_I$

FIGURE VI-2-2. HORIZONTAL IMPULSIVE SEISMIC MODEL

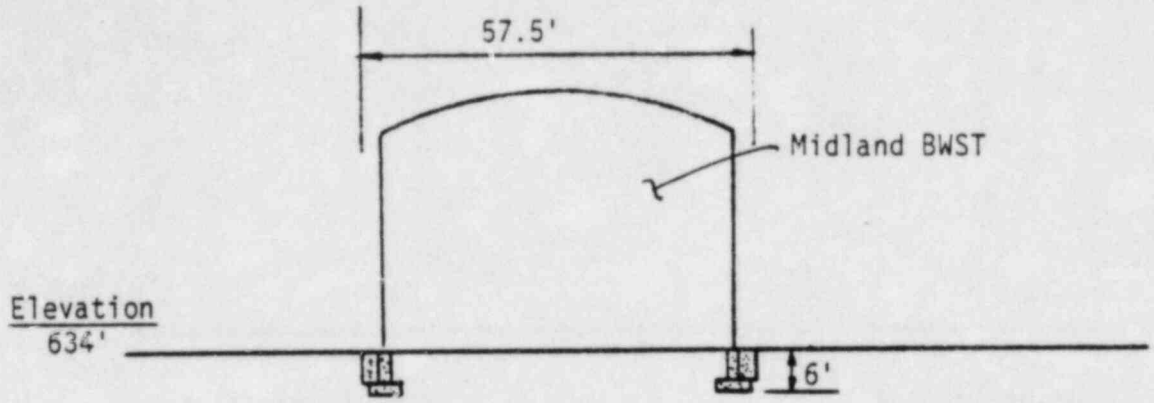

Fill — γ = 115 to 125 pcf; V_s = 500 to 575 fps; ν = 0.4 to 0.45; G_m = 0.9 to 1.2x10^3 ksf

615'

Fill — γ = 115 to 125 pcf; V_s = 750 to 850 fps; ν = 0.4 to 0.45; G_m = 2.0 to 2.7x10^3 ksf

610'

Original Till — γ = 115 to 135 pcf; V_s = 850 to 1290 fps; ν = 0.42 to 0.47; G_m = 2.7 to 7.0x10^3 ksf

553'

Original Till — γ = 135 pcf; V_s = 1690 to 2300 fps; ν = 0.42 to 0.47; G_m = 12 to 22x10^3 ksf

463'

Stiffness increases below 463'

FIGURE VI-2-3. ASSUMED SOIL PROFILE BENEATH MIDLAND BWST

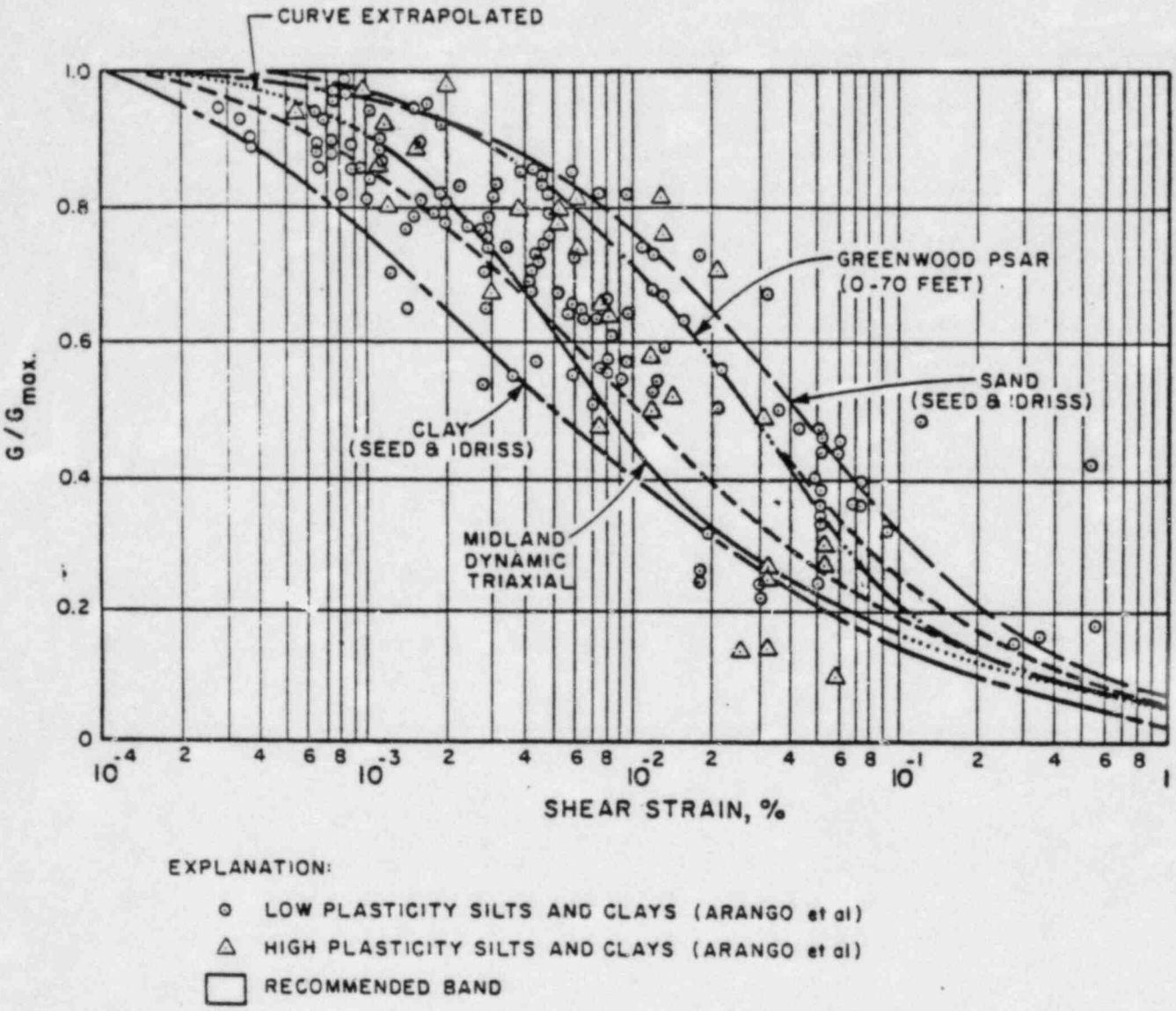

FIGURE VI-2-4. STRAIN DEGRADATION RELATIONSHIPS
(From Reference 10)

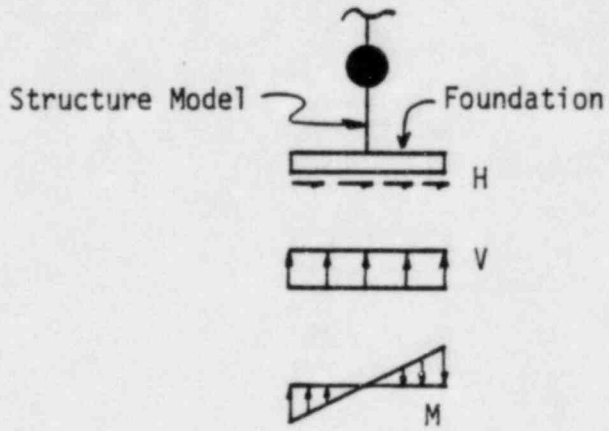

a. Soil Resistance Forces

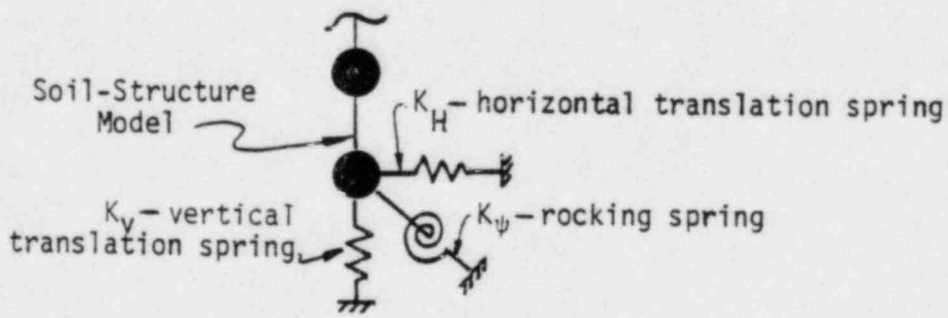

b. Equivalent Soil Springs

FIGURE VI-2-5. EQUIVALENT SOIL SPRING MODEL

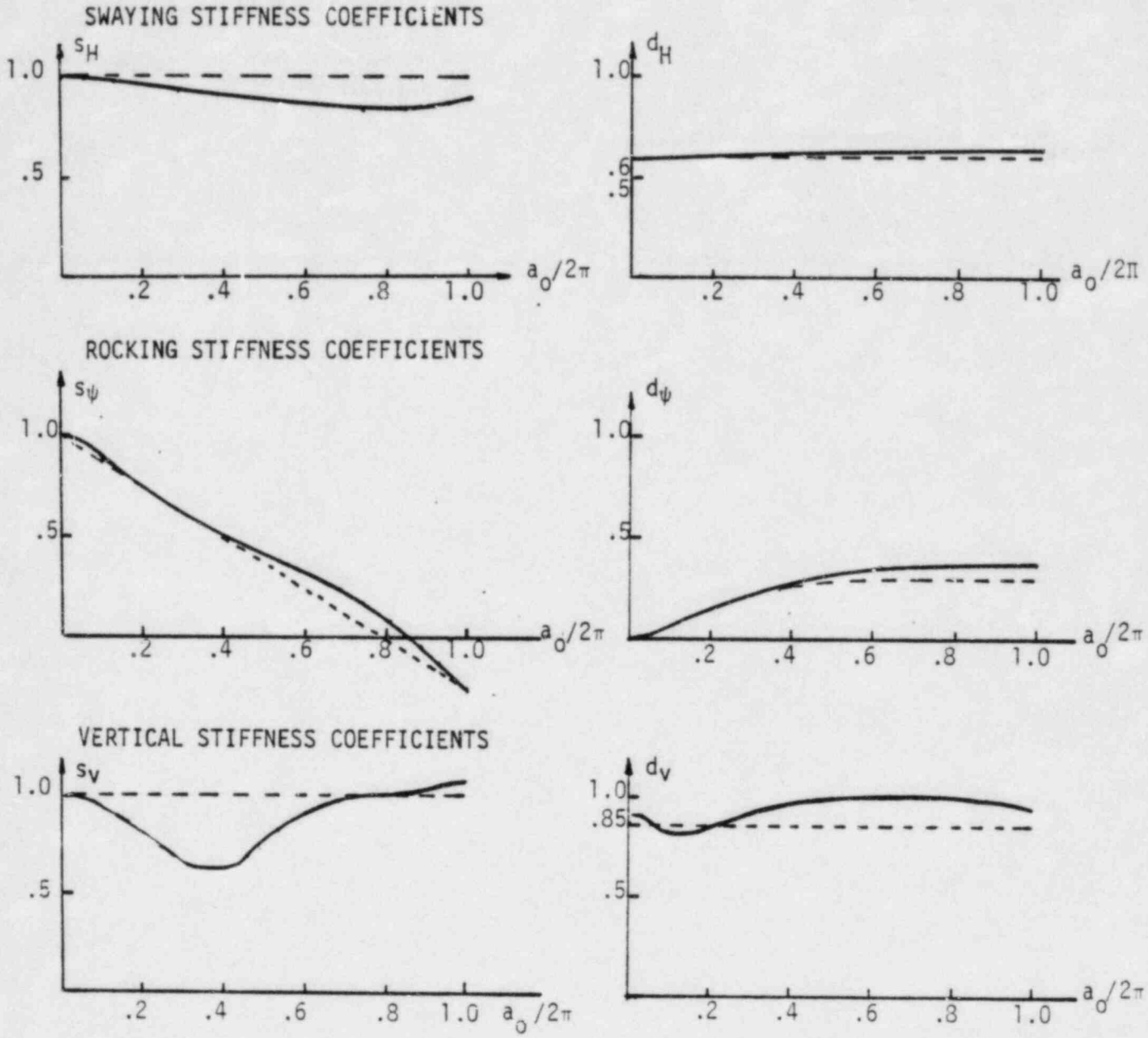

--- Approximation of Frequency-Dependent Stiffness Coefficients
(applicable to $\nu = 0.45$)

FIGURE VI-2-6. STIFFNESS COEFFICIENTS FOR A SURFACE FOOTING OVER AN ELASTIC HALF-SPACE (REFERENCE 5)

3. SEISMIC BEHAVIOR OF THE MIDLAND BWST

3.1 MODAL RESPONSES

The natural frequency, modal damping and corresponding spectral acceleration for the sloshing, impulsive and vertical response modes are summarized in Table VI-3-1. The horizontal sloshing mode is at a very low frequency such that the spectral acceleration is governed by the Housner response spectrum rather than the site specific spectrum. For horizontal impulsive response, there are two modes at frequencies below 33 hz with the first mode including participation of nearly all of the system mass and accounting for nearly all of the impulsive seismic response. The mode shapes for the impulsive response modes with the best estimate soil properties are illustrated in Figure VI-3-1. As mentioned in Chapter 2, the predominant response mode is at a frequency of 4.6 hz for the best estimate soil properties and includes coupled soil translation and rocking as well as structure response. From Table VI-3-1, it may be seen that the lower bound soil case leads to the largest spectral accelerations and thus, would produce the greatest seismic response. The evaluation of the tank seismic margin as discussed in the following chapter, is therefore based on seismic-induced loads as determined from analyses with lower bound soil properties. The tank itself is rigid in the vertical direction (i.e., vibration frequency greater than 33 hz). The lower frequencies shown in Table VI-3-1 are totally due to soil response in the vertical direction. The frequencies shown are in the amplified region of the response spectrum. However, at the very large damping appropriate for the vertical direction, there would be no amplification of the ground motion which, in the vertical direction, is 2/3 of the zero period horizontal ground acceleration of 0.15g.

3.2 BASE SHEAR, OVERTURNING MOMENT, AND VERTICAL SEISMIC LOADS AT TANK BASE

Seismic-induced base shear, overturning moment and vertical load at the top of the ring foundation are summarized in Table VI-3-2.

Individual response modes have been combined by the square-root-sum-of-squares (SRSS) method. As indicated by the spectral accelerations presented in Table VI-3-1, it is confirmed that the lower bound soil properties lead to the largest seismic-induced loads on the tank and its foundation. The maximum base shear is 539 kips, or about 20 percent of the tank and impulsive fluid weight. The maximum overturning moment at the base of the tank is 8154 foot-kips. The maximum vertical load on the foundation is 74 kips which is 10 percent of the weight of the tank (110 kips) plus the weight of a two foot wide ring of water, 32 feet high, directly above the ring wall footing (627 kips). These seismic induced loads have been used as the basis for the evaluation of the safety margin for the Midland BWST.

Other seismic response quantities of interest are the slosh height as determined from Equation 2-11 and the moment due to hydrodynamic pressures acting on the tank bottom as determined from Equation 2-4. The fluid slosh height has been computed to be approximately 1.0 feet. The dome roof of the BWST permits this level of sloshing without significant reduction of the free surface of the fluid. It is concluded that fluid sloshing during seismic response will not produce any damage to the tank roof.

The seismic-induced moment acting on the tank bottom computed in accordance with Equation 2-4 for the lower bound soil properties is 4930 foot-kips. A portion of the bottom pressure acts directly on the underlying soil and a portion of the bottom pressure is transmitted through the ring foundation and then into the soil. The amount of the bottom pressure moment acting on the two foot wide strip of tank bottom around the circumference of the tank directly above the foundation is 1350 foot kips. When evaluating the overturning moment on the ring wall, this 1350 foot-kips should be added to the overturning moment of 8154 foot-kips reported in Table VI-3-2 for the base at the tank shell. Thus, the total overturning moment on the ring wall is 9404 foot-kips. The remaining bottom pressure moment of 3580 foot-kips acts directly on the soil in the central region of the tank.

3.3 FLUID PRESSURES ON TANK SHELL

The hydrostatic and hydrodynamic pressures from the vertical earthquake component on the tank shell are triangular distributions given by:

$$P_{static} = \gamma y \tag{3-1}$$

$$P_{vertical} = \gamma y Sa_v \tag{3-2}$$

where γ = the fluid density

y = depth of fluid measured from the top of the fluid

Sa_v = the vertical spectral acceleration

The hydrodynamic pressures in the impulsive, P_1, and sloshing, P_2, modes over the height of the tank may be determined from Equations 2-3 ($V = 534k$) and 2-10 ($Sa_2 = .046g$), respectively. The resulting pressure distributions are illustrated in Figure VI-3-2. The hydrodynamic pressures are combined SRSS and then added absolutely to the hydrostatic pressure to obtain the total pressure on the tank shell. One may note that the seismic margin earthquake hydrodynamic pressures are small compared to the hydrostatic pressure.

TABLE VI-3-1

BWST DYNAMIC CHARACTERISTICS

Response		Frequency (Hz)	Modal Damping (%)	Spectral Acceleration (g)
Sloshing		0.24	0.5	0.046
Impulsive				
Lower Bound	Mode 1	3.7	20.0	0.214
	Mode 2	11.5	20.0	0.188
Best Estimate	Mode 1	4.6	20.0	0.211
	Mode 2	14.0	20.0	0.175
Upper Bound	Mode 1	5.6	20.0	0.210
	Mode 2	16.6	20.0	0.166
Vertical				
Lower Bound		4.3	88.0	0.100
Best Estimate		5.6	88.0	0.100
Upper Bound		7.2	88.0	0.100

TABLE VI-3-2

SUMMARY OF BWST SEISMIC-INDUCED FOUNDATION LOADS

		SME Seismic Response
Sloshing		
	Base Shear	72k
	Overturning Moment	1479 ft-k
Impulsive		
Lower	Base Shear	534k
	Overturning Moment	8019 ft-k
Best	Base Shear	520k
	Overturning Moment	7886 ft-k
Upper	Base Shear	507k
	Overturning Moment	7811 ft-k
Vertical	Vertical Load	74k
Combined Sloshing-Impulsive		
Lower	Base Shear	539K
	Overturning Moment	8154 ft-k
Best	Base Shear	525k
	Overturning Moment	8023 ft-k
Upper	Base Shear	512K
	Overturning Moment	7950 ft-k
Maximum Response		
	Base Shear	539k
	Overturning Moment	8154 ft-k
	Vertical Load	74k

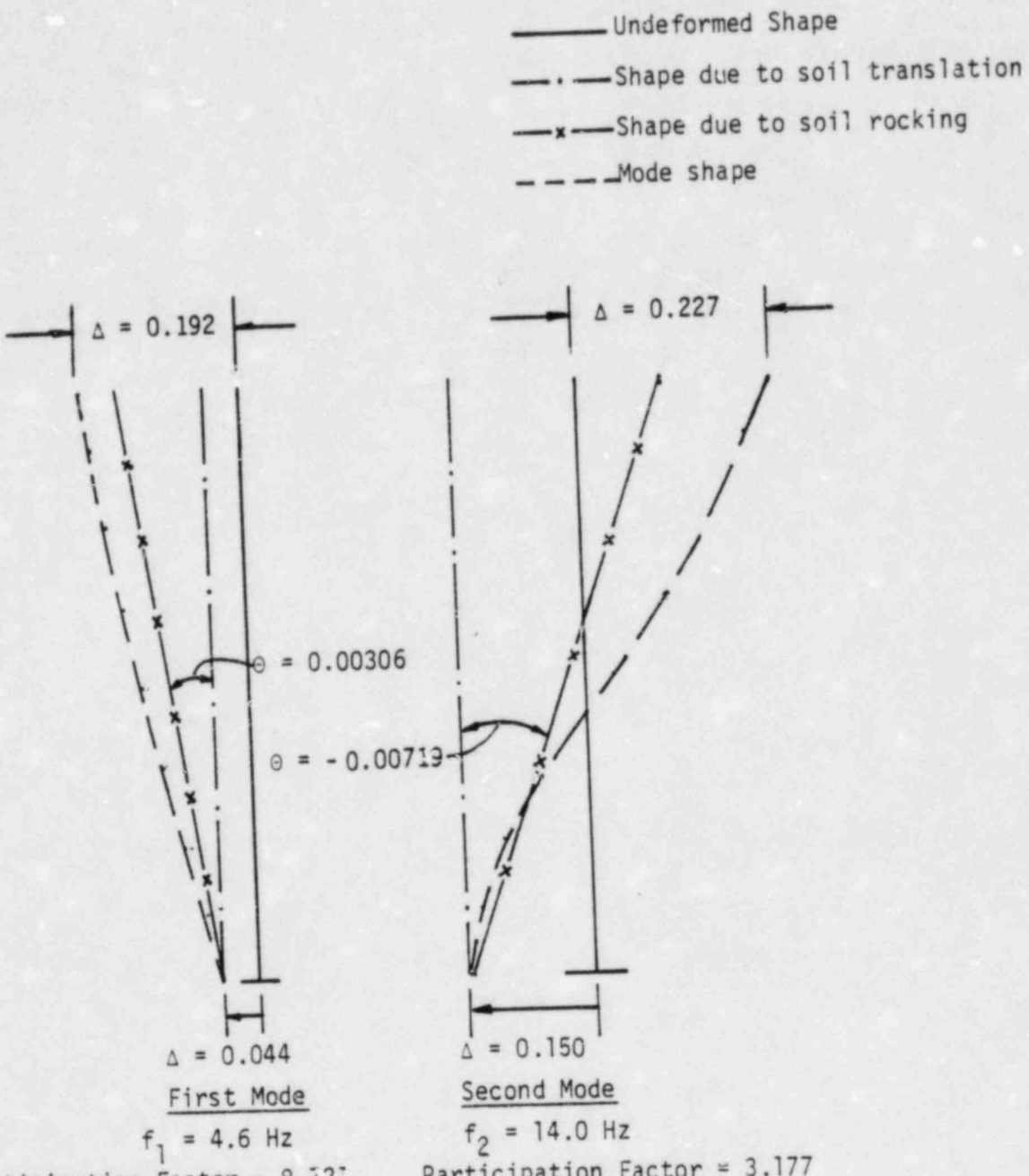

FIGURE VI-3-1. MODAL PROPERTIES OF BWST TANK - IMPULSIVE WATER - SOIL-SPRING MODEL (BEST ESTIMATE SOIL)

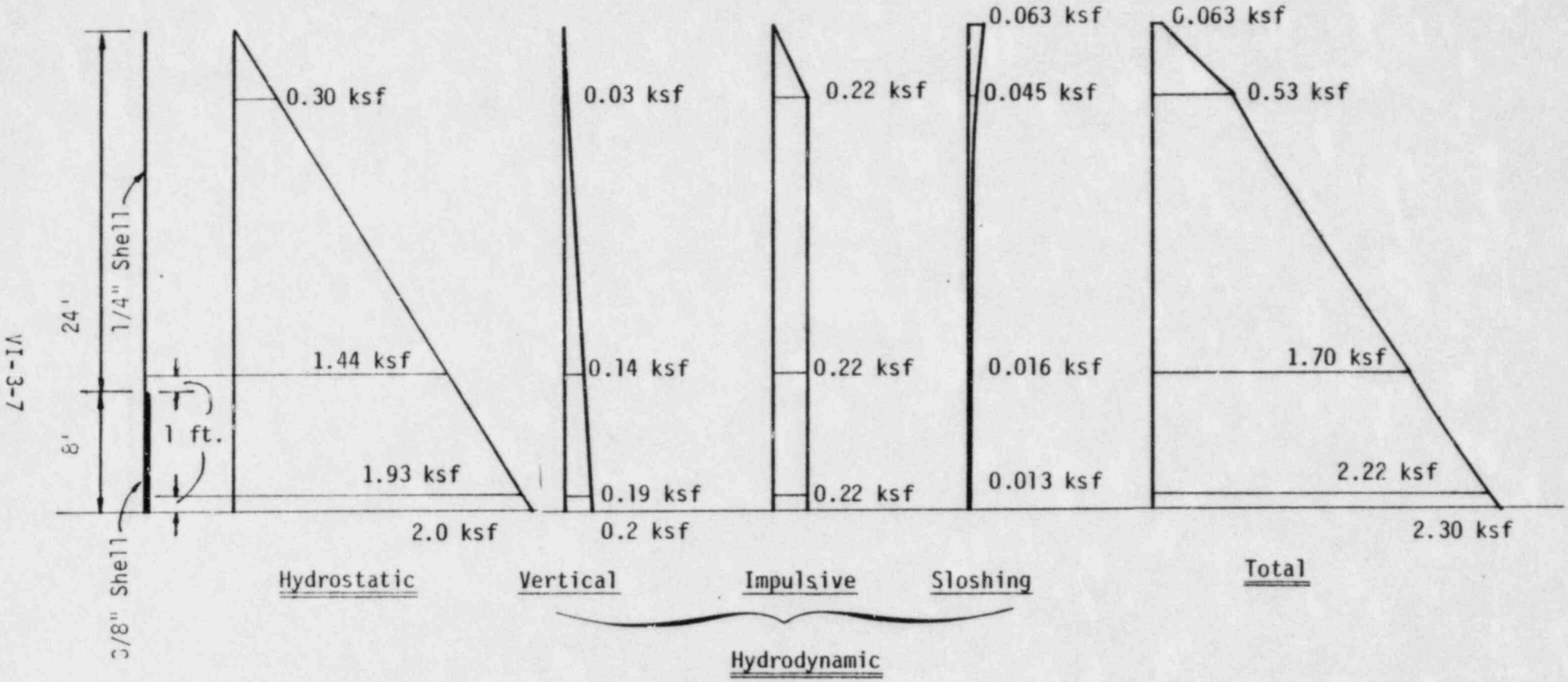

FIGURE VI-3-2. BWST HYDROSTATIC AND HYDRODYNAMIC PRESSURE DISTRIBUTION

4. CODE MARGIN FOR SEISMIC MARGIN EARTHQUAKE

4.1 GENERAL

The margins against the applicable code criteria are reported for the seismic margin earthquake in this chapter. These margins are determined for the concrete foundation, the tank, and its anchorage to the ring wall.

To determine the code margin, the seismic margin earthquake (SME) is substituted for the Safe Shutdown Earthquake (SSE) in the applicable code equations.

4.2 FOUNDATION CODE MARGIN

4.2.1 Basic Code and Seismic Margin

For the concrete foundation, the applicable code for the seismic margin review is taken to be ACI-349-76 as supplemented by US NRC Regulatory Guide 1.142. For the SME, the governing load combination equation is:

$$U = DL + T + F + L + H + SME \qquad (4\text{-}1)$$

where
- DL = dead load
- T = differential settlement
- F = hydrostatic pressure from ground water
- L = live load
- H = lateral earth pressure
- SME = Seismic Margin Earthquake

However, Bechtel Corporation has already design-checked the concrete foundation for the OBE and a foundation SSE level of 1.5 times the FSAR SSE level to this same design code (Reference 12). This design check of

the foundation was performed by applying inertial loads at the foundation level obtained from a tank seismic analysis to a finite elment model of the concrete foundation including the ring wall, footing, ring beam, the dowels between the ring beam and ring wall, and the valve pit. The most critical load combination equation for this design check was:

$$U = 1.4DL + 1.4T + 1.4F + 1.7L + 1.7H + 1.9\ OBE \qquad (4\text{-}2)$$

For this load combination, Table 2 of Addendum No. 1 of Reference 12 shows a minimum code margin (code capacity divided by applied load) of 1.02. As a result, the minimum code margin for Equation 4-1 is:

$$CM = 1.4(1.02) = 1.43$$

The OBE overturning moment applied to the ring wall was 11,061 ft-kips minus 3359 ft-kips or 7702 ft-kips (Table 4 of Reference 12). Section 3.2 defines an SME overturning moment of 9504 ft-kips. Comparing Equations 4-1 and 4-2 indicates a conservative minimum seismic margin for Equation 4-1 of:

$$F_{SME} = \left(\frac{7702}{9504}\right)\ (1.9)(1.02) = 1.57$$

Note that the seismic margin F_{SME} is the factor by which the SME could be increased with other loads held constant before response at the code capacity in accordance with Equation 4-1 is reached. Thus, since the concrete foundation has already been design-checked for Equation 4-2 with a conservative OBE overturning moment, it is unnecessary to check this foundation for the SME. Simply by comparing the SME overturning moment to 1.9 times the conservative OBE overturning moment, one shows a minimum seismic margin of 1.57. The actual seismic margin for the foundation is much larger than 1.57 as the code margin of 1.02 for Equation 4-2 is primarily due to differential settlement. A very large seismic margin will be demonstrated by calculations of the concrete foundation seismic behavior as described later in this chapter.

4.2.2 Additional Foundation Capacity Checks

Even though extrapolation of the design-check load combinations indicate a minimum seismic margin for the SME combined with dead load, settlement, hydrostatic pressure, live load, and lateral earth pressures of at least 1.57, some additional seismic margin checks have been performed on the concrete foundation and supporting soil. These checks have been on:

a) Soil bearing capacity under the footing
b) Tank sliding
c) Uplift
d) Concrete foundation capacity checks without differential settlement

These checks were performed to provide independent verification of the seismic capability of the foundation to withstand the SME. These checks considered dead load and SME only. Note that in addition to the above items, bending and torsion of the ring beam during seismic response have been considered. However, for these behavior modes, it is judged that foundation loads will be transmitted directly into the surrounding soil and the seismic margin will be very large without capacity calculations.

4.2.2.1 Soil Bearing Capacity

Compressive forces due to the weight of the tank, contained fluid and foundation and due to seismic-induced loadings can potentially lead to a bearing failure of the underlying soil. Based upon conservatively considering the weight of the tank shell and roof, the weight of the water directly above the foundation, the weight of the concrete foundation (ring wall and new ring beam), the weight of soil above footing as well as the seismic-induced load on the tank bottom plate, seismic-induced load due to vertical earthquake motion, and the seismic-induced load on the tank shell due to the overturning moment, the soil bearing pressure distribution (at the most critical section) shown in Figure VI-4-1 was obtained. The average bearing pressure is 3.26 ksf on the footing

cross-section with a maximum value of 3.96 ksf. The average bearing pressure of 3.26 ksf is comprised of 2.12 ksf due to static loading and 1.14 ksf due to the SME.

For soil beneath the ring wall subjected to combined static and earthquake loadings, the net bearing capacity is reported to be 8.05 ksf in Reference 17. Note that the value given above, is net bearing capacity defined as the pressure that can be supported at the base of the footing in excess of the pressure at the same level due to the surrounding surcharge. Considering a footing depth of six feet and a soil density of 115 pcf, the bearing factor of safety for the SME would be:

$$F.S. = \frac{8.05 \text{ ksf}}{3.26 \text{ ksf} - 6 \text{ ft}(0.115 \text{ kcf})} = 3.13$$

For design, FSAR Subsection 2.5.4.10.1 (Reference 9) specifies a minimum factor of safety of 2.0 for operating loads plus SSE. Thus, the "code" margin is:

$$CM = \frac{3.13}{2.0} = 1.57$$

The factor F_{SME} by which the SME ground motion would have to be multiplied to reach code allowable stress is:

$$F_{SME} = \frac{(8.05/2.0)-2.12 + 6(0.115)}{1.14} = 2.28$$

4.2.2.2 Tank Sliding

The seismic-induced base shear from Table VI-3-2 is 539 kips. This horizontal force will be transferred into the underlying soil by friction. The weight of the tank and contents is approximately 4,350 kips. Considering vertical earthquake effects, the effective weight could be reduced to about 4,180 kips at the time of maximum base shear. Therefore, the required friction coefficient to resist sliding is 539/4,180 = 0.13.

The tank bottom is not flat or particularly smooth. The tank bottom consists of 1/4 inch plates joined together by welds at lap joints. In addition, the tank bottom is designed to be higher in the center than at the tank walls to facilitate drainage. As a result, the friction coefficient is governed by the cohesion and angle of internal friction of the soil. The soil directly beneath the tank bottom is a granular fill material for which a cohesion value of zero and an angle of internal friction, ϕ, of 30 degrees are conservative. These properties correspond to a friction factor of about 0.36 (conservatively estimated as tan $2/3\,\phi$) which would provide a factor of safety against tank sliding of 2.8.

Based upon a required factor of safety against sliding of 1.1 (appropriate for SME level), the "code" margin is:

$$CM = \frac{2.8}{1.1} = 2.5$$

The factor, F_{SME}, is also 2.5 since seismic is the only loading causing sliding.

4.2.2.3 Foundation Uplift Capacity

The weight of the steel tank, the concrete foundation, and the fluid and soil above this foundation are all available to resist uplift due to seismic-induced overturning moment. Considering the weight of the original ring wall and footing, the new ring beam, the tank shell and roof, and the water and soil directly above, the resulting static pressure

on the soil beneath the 4-foot-wide footing is 2.12 ksf computed as shown in Figure VI-4-2. Considering vertical earthquake and negative hydrodynamic pressures which reduce the hydrostatic pressures on the tank bottom plate above the footing, this pressure can be reduced to 1.87 ksf during the SME as shown in Figure VI-4-2. For this calculation, it is assumed that 40% of the peak negative vertical earthquake effects act concurrently with the maximum overturning moment. This assumption is consistent with the SRSS of earthquake components.

The overturning moment that would overcome the minimum compressive pressure of 1.87 ksf such that uplift of the ring foundation is initiated is 15,885 ft-kips as computed in Figure VI-4-2. Compared to the SME seismic-induced overturning moment of 8,154 ft-kips (Table VI-3-2), the foundation uplift factor of safety is:

$$F.S. = \frac{15,885}{8,154} = 1.95$$

Foundation uplift does not constitute a failure mode for the tank. Thus, a minimum factor of safety of 1.0 should be acceptable for the SME. In this case, the code margin is:

$$CM = 1.95$$

The factor F_{SME} by which the SME earthquake would have to be multiplied to lead to an uplift factor of safety of 1.0 is:

$$F_{SME} = \frac{15885\left(\frac{2.12}{1.87}\right)}{8154 + 15885\left(\frac{2.12-1.87}{1.87}\right)} = 1.75$$

The seismic margin factor, F_{SME}, is less than the code margin, CM, because the vertical earthquake component increases as the horizontal ground motion increases. Thus, the vertical earthquake component reduces the capacity to withstand horizontal overturning moments without uplift.

4.2.2.4 Concrete Foundation Capacity Checks without Differential Settlement

The basic code and seismic margin for the concrete foundation has been presented in Section 4.2.1. This foundation design check is extremely conservative as it is predominantly affected by differential settlement and not by seismic loadings. It is unlikely that the conservative 40-year predicted differential settlements occur at the same time as the SME. Furthermore, settlement stresses are displacement controlled (i.e., self-limiting), and are not expected to contribute to failure during an earthquake. Therefore, the following analysis which neglects stresses due to differential settlement is considered to give more realistic values for the failure capacity of the concrete foundation.

The reinforced concrete tank foundation consists of the original ring wall and footing and the new ring beam as illustrated in Figure VI-1-3. The foundation was checked for the two seismic loading conditions illustrated in Figure VI-4-3: 1) bending of the footing; and 2) hoop tension of the ring beam due to outward pressure of the entrapped soil within the foundation ring resulting from vertical loads on this soil. As mentioned previously, bending and torsion of the ring beam during seismic excitation were also considered but it was judged that for these behavior modes the seismic loads would be transmitted directly into the surrounding soil such that the seismic response of the ring beam in bending and torsion would be very small. The concrete foundation, including both the original ring wall and footing and the ring beam added during foundation remedial work, are made of concrete with minimum unconfined compression strength, f'_c of 4000 psi and reinforcing bars with minimum yield strength of 60,000 psi.

The loading shown in Figure VI-4-3a imposes a bending moment onto the 1.25-foot-long footing extension of 2.42 ft-kips/ft. The ACI 349-76 ultimate moment capacity of this footing extension is 28.3 ft-kips/ft. Thus, the code margin of this footing extension is:

$$CM = \frac{28.3}{2.42} = 11.7$$

The soil entrapped within the ring foundation is subjected to vertical loads due to the water weight as well as due to the maximum hydrodynamic pressure from vertical seismic and overturning moment bottom pressures acting on the tank bottom. This loading, acting on the entrapped soil, results in the ring beam being in hoop tension due to lateral pressure resulting from this vertical surcharge (Figure VI-4-3b). (Only the tensile steel within the new ring beam was considered effective in withstanding this loading). It has been conservatively assumed that the lateral pressure resulting from the vertical load is one-half of the vertical loading. In evaluating the foundation for this loading, the constraint from the soil outside the ring beam has been conservatively ignored. By this extremely conservative approach, there is a factor of safety of 11.3 against yielding of the foundation circumferential reinforcement. Thus,

$$CM = 11.3$$

4.3 ANCHOR BOLT CODE MARGIN

Anchor bolt capacity is governed by the lesser of:

1. Bolt pullout from the concrete
2. Tensile capacity of the bolt
3. Tensile capacity of ring wall to footing connection

Anchor bolts are spaced at about equal 49 inch intervals around the tank circumference. The 1.5 inch diameter A36 anchor bolts extend into the concrete ring wall foundation 24 inches as is shown in Figure VI-1-3. Each bolt has a 2.5 inch thick, 6 inch square anchor head plate at its end about 22 inches below the top of the ring wall.

The pullout capacity of the bolt and embedment plate has been evaluated in accordance with ACI-349 provisions. By this approach, the capacity is evaluated based on a uniform tensile stress of $4 \phi \sqrt{f'_c}$ acting on an effective stress area which is defined by the projected area of a stress cone radiating toward the surface of the footing from the bearing edges of the anchor head (see Figure VI-4-4). The effective area is limited by overlapping stress cones, by the intersections of cones with concrete surfaces, by the bearing area of the anchor head and by the ϕ embedment depth of the anchor head. The inclination angle for calculating projected areas is taken to be 45 degrees. For this evaluation, the factor has been taken to be 0.65 which corresponds to the case in which the embedded anchor head does not extend beyond the far face reinforcement of the footing. It should be noted that the ring beam to be added around the outside of the original ring wall foundation will provide confinement to the original ring wall to prevent failure due to lateral bursting forces at an anchor head which is the concern of Paragraph B.5.1.1 of the code. However, this ring beam does not increase the effective stress area as the original rng wall and ring beam are not tied together until a depth of 18 inches which is almost equal to the anchor bolt embedment length (see figure 1-3).

The allowable load for the bolt itself is based on AISC Manual of Steel Construction, Part 2 criteria. Section 1.5.2.1 of the AISC Code states that for tension on the nominal bolt area, the allowable stress is 1/3 of the ultimate tensile stress. Further, Part 2 of the AISC Code allows an increase factor of 1.7 for ultimate capacity. Thus, for 1-1/2 inch diameter A36 bolts with an ultimate tensile strength of 58 ksi, the allowable ultimate load capacity is 57.4 kips.

The construction joint between the original ring wall and underlying footing is crossed by #7 bar reinforcing steel spaced at 12 inches on each face. Thus, a total of 4.9 square inches of 60 ksi yield strength reinforcing steel crosses this joint for each anchor bolt. The ultimate tensile capacity of this construction joint is 294 kips per anchor bolt.

Thus, the anchor bolt capacity is governed by the tensile capacity of the bolts and is 57.4 kips.

The maximum uplift force on the bolts is computed from the seismic-induced overturning moment of 8154 ft-kips. Since the tank shell is in compression due to dead weight, a portion of this moment relieves the compressive stresses and the remaining moment goes into the bolt forces. In Figure VI-4-5, it is illustrated that the maximum bolt force is 13.2 kips. This force is made up of 15.7 kips SME overturning moment tensile force minus 2.5 kips of dead load compression which must be overcome before anchor bolt tensions develop.

Reference 15 reports a maximum anchor bolt tension of 6.0 kips due to combined settlement and dead load. Thus, the total anchor bolt tension due to dead load, settlement, and the SME is:

$$T_a = 15.7 \text{ kips} + 6.0 \text{ kips} = 21.7 \text{ kips}$$

This anchor bolt load is compared to the code allowable capacity in Table VI-4-1.

The minimum anchor bolt code margin is:

$$CM = \frac{57.4 \text{ kips}}{21.7 \text{ kips}} = 2.65$$

The factor, F_{SME}, by which the SME ground motion would have to be multiplied to reach code allowable stress is:

$$F_{SME} = \frac{57.4-6.0}{15.7} = 3.27$$

4.4 TANK CODE MARGIN

4.4.1 Governing Codes and Standards

The BWSTs are designed and code stamped to the ASME code, Section III, Nuclear Power Plant Components, Subsection NC, Class 2 Components, Paragraph NC3300, Design of Vessels. The 1974 code, with no

addenda, are applicable and Code Case 1607-1 is applicable for upset, emergency and faulted condition stress allowables. The API 650 code (Reference 13) is also specified for design. In cases of conflict, the ASME Code governs.

The basic design is conducted using API-650 criteria since NC3300 of the ASME code does not specifically address flat-bottom storage tank designs. NC3800 does provide criteria for flat-bottom storage tanks and is essentially identical to API-650. The ASME code stress acceptance criteria from Code Case 1607-1 is used for evaluation of the OBE and SSE events.

Under the governing criteria, the following stress intensities are allowed.

Loading Condition	Primary Membrane	Primary Local Membrane plus Primary Bending
Design and Normal	S	1.5S
Upset	1.1S	1.65S
Emergency	1.5S	1.8S
Faulted	2.0S	2.4S
Testing	1.25S*	1.87S**

* Not to exceed 0.9 S_y
** Not to exceed 1.35 S_y

The allowable stress intensity, S, is 15.7 ksi for 304 L stainless steel. Secondary stresses do not require evaluation for Class 2 components designed by rule (NC3300 criteria). Minimum specified yield strength, S_y, is 25 ksi.

For the code margin check, SME response is added to that from dead load, fluid hydrostatic pressure, and settlement with the resultant stresses compared to faulted condition allowables. These allowables are

31.4 ksi for primary membrane and 37.7 ksi for primary local membrane plus primary bending. Whenever dead weight reduces the effect of seismic loads, only 90 percent of the dead weight stress is included.

Settlement stresses added to stresses resulting from the SME are obtained from the Addenda to Reference 15.

4.4.2 Tank Shell Hoop Stress

Hoop tensile stresses in the tank shell occur due to internal pressure on the tank wall from the contained fluid. Internal pressures are due to the static head of fluid plus hydrodynamic pressures resulting from seismic response in the sloshing, impulsive and vertical modes. Hoop stresses are evaluated for both the 3/8-inch-thick shell and for the 1/4-inch thick shell. The Code (Reference 13) requires hoop stress to be evaluated at an elevation which is one foot above the bottom of the shell course under consideration. For hydrostatic and hydrodynamic pressures, the hoop stress is given by $\sigma = pR/t$ where p is pressure, R is tank radius and t is tank wall thickness. The hydrostatic and SME pressures were presented in Figure VI-3-2. Based upon these pressures, the SME seismic and hydrostatic hoop stresses are presented in Table VI-4-1. These stresses are compared to a primary membrane stress of 31,400 psi.

The minimum hoop stress code margin is:

$$CM = \frac{31400 \text{ psi}}{14733 \text{ psi}} = 2.13$$

The factor, F_{SME}, by which the SME ground motion would have to be multiplied to reach code allowable stress is (see Table VI-4-1 for individual response values):

$$F_{SME} = \frac{31400 - 12480}{2253} = 8.40$$

4.4.3 Longitudinal Buckling of Tank Shell

The maximum SME overturning moments at the base of the tank and eight feet above the base of the tank (i.e., at the bottom of the 1/4-inch section) are 8154 and 4358 ft-kips, respectively. Assuming a linear variation of stress over the tank diameter, the corresponding SME longitudinal compression stresses in the 3/8-inch and 1/4-inch shell sections are 853 and 684 psi, respectively. Respective dead load compression stresses are 15 and 18 psi which are negligible when combined SRSS with the horizontal overturning moment stresses. Reference 15 reports the summation of dead load and maximum settlement compressive stresses to be 1066 and 1164 psi for the 3/8-inch and 1/4-inch shell sections, respectively. These stresses are tabulated in Table VI-4-1.

For the large diameter, thin-wall storage tank, buckling will occur in the elastic range. The ASME Code buckling criterion for axially loaded cylinders nominally contains a safety factor of 3 for sustained design loads. The ASME Code specifies in Article NC-3000 that the maximum allowable compressive stress to be used in the design of cylindrical shells shall be the lesser of:

a) The allowable S value given in Tables I-7.0 of the Code

b) The value of B determined from the applicable chart in Appendix VII of the Code.

For the case under consideration, the latter criterion governs.

The value of B for elastic buckling in Appendix VII can be obtained with a higher degree of accuracy by using the design formula shown below, taken from the 1977 ASME Code.

$$B = \frac{0.0625\ Et}{R} \qquad (4\text{-}3)$$

where

E = modulus of elasticity
t = shell thickness
R = inside radius of shell

This formula applies to the linear portion of the buckling curves in Appendix VII and is applicable for the BWST analysis. The buckling allowables, B, for the design and normal loading conditions are therefore:

B = 1417 psi (for 1/4" shell)

B = 2126 psi (for 3/8" shell)

Based on Code Case 1607-1, the Faulted Condition allowables can be increased by a factor of 2.0 for primary membrane stresses. Thus, the buckling allowables for faulted conditions, $\sigma_{cr} = 2B$, are:

σ_{cr} = 2834 psi (1/4" shell)

σ_{cr} = 4252 psi (3/8" shell)

These allowable capacities are compared with the SME, dead load and settlement applied stresses in Table VI-4-1.

The buckling code margin is controlled by the 1/4 inch shell section for which the buckling allowable is 2834 psi and the combined seismic, dead load and settlement stress is 1848 psi (see Table VI-4-1). Thus, the minimum code margin for buckling is:

$$CM = \frac{2834}{1848} = 1.53$$

The factor, F_{SME}, by which the SME ground motion would have to be multiplied to reach code allowable stress is:

$$F_{SME} = \frac{2834-1164}{684} = 2.44$$

where 1164 psi is the tank shell compression stress due to settlement and dead load and 684 psi is the SME tank shell compressive stress (see Table VI-4-1).

4.4.4 Local Membrane Stress in Shell at the Bolt Chairs

Bolt chairs attach to the tank shell at approximately one foot above the tank bottom as shown in Figure VI-4-6. Anchor bolt tension acting on these bolt chairs produce local membrane hoop stresses in the tank shell due to the eccentric lever arm of the anchor bolt relative to the tank shell centerline. Section 5.3 of Reference 15 computes local membrane hoop stresses of 13,200 psi due to a 31.31 kip anchor bolt tension based upon the methods of Reference 16. Thus, local membrane hoop stresses, $\sigma_{\ell m}$, are given by:

$$\sigma_{\ell m} = \frac{13200 \text{ psi}}{31.31 \text{ kips}} T_a = 422 \frac{\text{psi}}{\text{kip}} \cdot T_a \qquad (4\text{-}4)$$

where T_a is the anchor bolt tension. These local membrane hoop stresses which are a function of the anchor bolt tension add to the overall hoop tensile stresses reported in Table VI-4-1 for the 3/8-inch shell at this same location.

The total local membrane hoop tension due to the SME is:

$$\sigma_{\ell m_{SME}} = 1676 \text{ psi} + 422 \text{ psi/kip}(15.7 \text{ kips}) = 8301 \text{ psi}$$

Due to dead load, hydrostatic pressure, and settlement, this stress is:

$$\sigma_{\ell m_{DW+S}} = 11177 \text{ psi} + 422 \text{ psi/kip}(6.0 \text{ kips}) = 13709 \text{ psi}$$

These stresses are combined in Table VI-4-1 and compared to the primary local membrane plus primary bending allowable stress of 37,700 psi.

The local membrane stress code margin is:

$$CM = \frac{37700 \text{ psi}}{22010 \text{ psi}} = 1.71$$

and the factor, F_{SME}, is:

$$F_{SME} = \frac{37700 - 13709}{8301} = 2.89$$

4.5 BOLT CHAIR BENDING

The top plate of the bolt chair is subjected to bending due to anchor bolt tension. Original bolt chair bending design-analysis was conducted by the conservative design method contained in Reference 14. The method assumes that a beam of width, f, equal to the edge distance from the hole to the plate outside edge carries one-third of the total bolt load. Figure VI-4-7 shows the analytical model. In this figure, it is shown that the beam span is g, the top plate thickness is c and the loading occurs over a width equal to the bolt diameter, d. For a total bolt load, P, the maximum top plate stress, σ, is given by:

$$\sigma = \frac{P}{f c^2} (0.375g - 0.22d) \qquad (4\text{-}5)$$

The computed stress was to be held to the faulted condition primary bending allowable stress of 37,700 psi (Section 4.4.1). Based upon this approach, the total faulted condition bolt capacity would be:

(Conservative Design Method): $P_{CAP} = 23.6$ kips

The above represents a very conservative capacity estimate based upon a conservative procedure used in design.

The capacity can be more accurately evaluated using the ASME Code, Section III, Nuclear Power Plant Components, Subsection NF, Component Supports, Paragraph NF 3200, Design of Class 1 Component Supports, 1980. It is acceptable to use Class 1 design criteria to evaluate the supports on a Class 2 tank because Class 1 criteria are more stringent than Class 2. Paragraph NF 3220, Design of Plate and Shell-Type Supports by Analysis, allows the Level C Service Limits (comparable with the 1974 Emergency Loading Condition) to be establisned for primary membrane plus bending by the limit analysis method. The maximum allowable value of the combined stresses by this method is 0.8 C_L where C_L designates the collapse load calculated on the basis of the lower bound theorem of limit analysis using the yield strength value for Type 304 L stainless steel of 25 ksi. In our judgment, component supports should not be allowed to exceed 0.8 C_L for Level D Service Limits (Faulted Loading Condition). Therefore, this Level C limit will also be applied to Level D.

The collapse load is determined by a yield-line analysis of the bolt chair top plate. The applicable yield-line (collapse mechanism) is shown in Figure VI-4-8. The bolt load bears on the two least deformed points of the top plate in its yield mechanism under the bolt nut. These points are shown in Figure VI-4-7 at a distance R_{eff} from the bolt center. Lines ①, ②, ③ and ④ repesent yield hinges. The plastic moment capacity of hinge ① is governed by two (2) times the plastic moment capacity of the tank wall which is less than the plastic moment capacity of the top plate. The plastic moment capacity of hinge ② is governed by the vertical gusset plate plastic moment capacity, Thus,

$$M_{①} = \frac{(25\ ksi)(2)(0.375\ in)^2}{4} = 1.76\ in\text{-}kips/in$$

$$M_{②} = \frac{(25\ ksi)(0.5\ in)^2}{4} = 1.56\ in\text{-}kips/in$$

$$M_{③} = M_{④} = \frac{(25\ ksi)(0.625\ in)^2}{4} = 2.44\ in\text{-}kips/in$$

The collapse load capacity is given by:

$$C_L = \frac{2}{(g/2-R_{eff})} \left\{ M_{①} (g/2) \cot\alpha \right. \qquad (4\text{-}6)$$

$$\left. + M_{②}(b) + M_{③}(\ell\sin\alpha + f) + M_{④}(\ell \cos\alpha\cot\alpha) \right\}$$

where

$$\cot\alpha = \frac{(g/2) - R_H \cos\beta}{a - R_h \sin\beta}$$

$$\ell = \frac{a - R_H \sin\beta}{\sin\alpha}$$

The angle β is varied until the minimum value of C_L is obtained from Equation 4-6. The capacity C_L is insensitive to the angle β between 0 and 55 degrees but is a minimum at an angle β of about 25 degrees. Ignoring any benefit from the bolt nut in spreading the load, R_{eff} is conservatively underestimated to be 0.834 inches or less than the hole radius. With this value of R_{eff} and a β angle of 25 degrees, the collapse load capacity is:

$$C_L = 40.6 \text{ kips}$$

The code capacity, P_{CAP}, based upon the collapse load is 0.8(40.6 kips) or 32.5 kips. Thus:

(Collapse Load Approach): $P_{CAP} = 32.5$ kips

The anchor bolt loads were presented in Section 4.3 and are summarized in Table VI-4-1. Comparing capacity to load leads to a minimum code margin for the bolt chair of:

$$CM = \frac{32.5 \text{ kips}}{21.7 \text{ kips}} = 1.50$$

and a multiplication factor on the SME of:

$$F_{SME} = \frac{32.5 - 6.0}{15.7} = 1.69$$

The 3/8-inch fillet weld between the bolt chair gusset plates and the tank shell was also checked and found to be not governing the bolt chair capacity.

TABLE VI-4-1

STRESS COMBINATIONS - SME + DW + SETTLEMENT

Parameter	Seismic Response from SME (Faulted Condition)	DW + Settlement Response	Total Response	Allowable Response
Tensile Hoop Stress in 3/8" Shell	1676 psi	11,177 psi	12,853 psi	31,400 psi
Tensile Hoop Stress in 1/4" Shell	2253 psi	12,480 psi	14,733 psi	31,400 psi
Compression Stress in 3/8" Shell	853 psi	1,066 psi	1,919 psi	4,252 psi
Compression Stress in 1/4" Shell	684 psi	1,164 psi	1,848 psi	2,834 psi
Local Membrane Stress in Shell at Bolt Chair	8301 psi	13,709 psi	22,010 psi	37,700 psi
Bolt Chair Top Plate Bending Load	15.7 kips	6 kips	21.7 kips	32.5 kips
Anchor Bolt Load	15.7 kips	6 kips	21.7 kips	57.4 kips

SME = Seismic Margin Earthquake
DW = Deadweight + Hydrostatic Pressure Loads

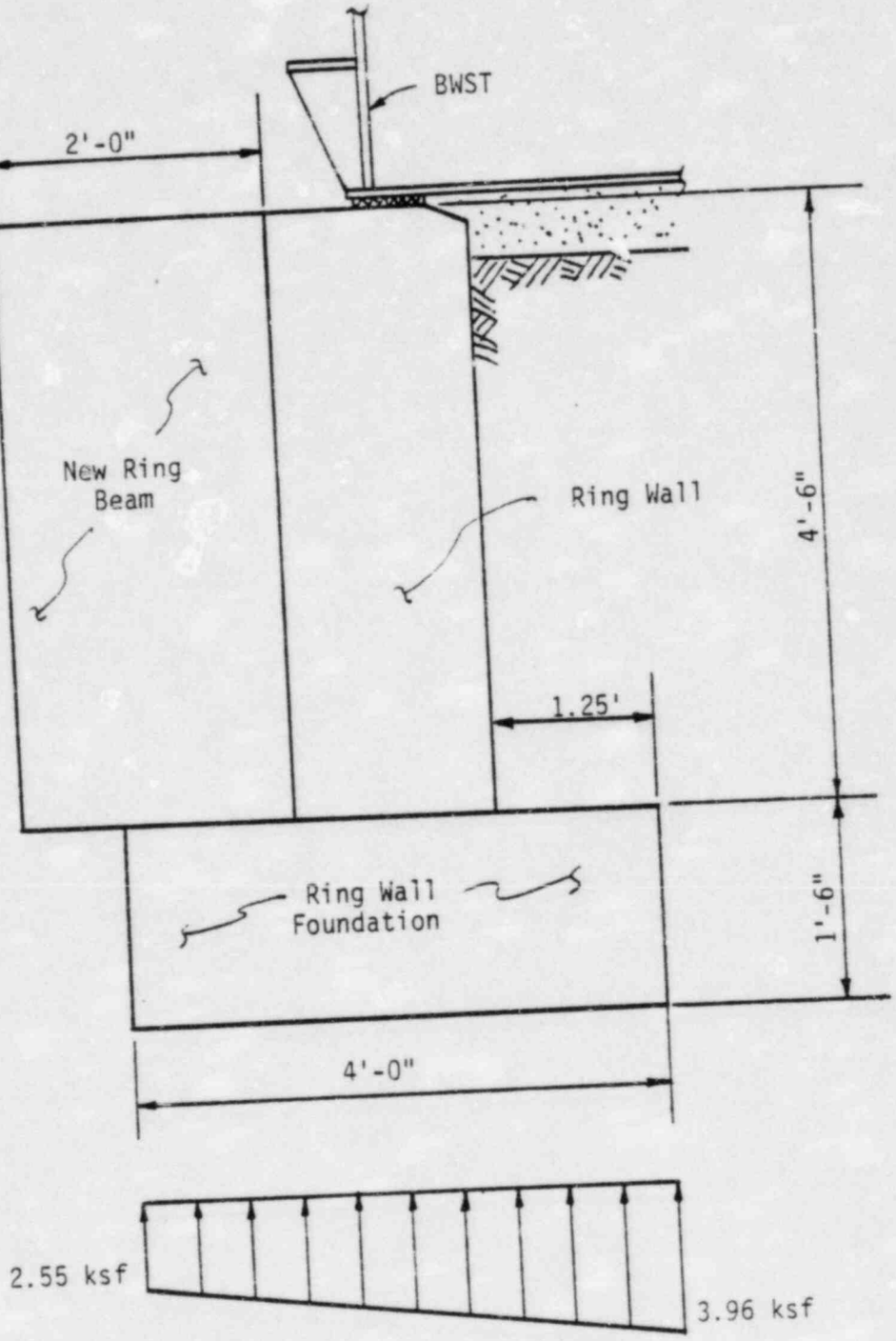

FIGURE VI-4-1. SOIL BEARING PRESSURE DISTRIBUTION

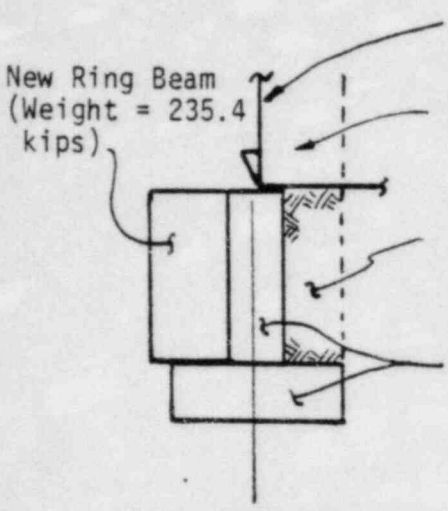

Tank Shell (Weight = 110.3 kips)

Fluid Annulus above Footing (Weight = 527.3 kips)

Entrapped Soil (Weight = 100.1 kips)

Original Ring Wall and Footing (Weight = 312.4 kips)

TOTAL WEIGHT = 1386 kips

Soil Pressure Due to Dead Load

$$= \frac{1386}{\pi(28^2-24^2)} = \underline{2.12 \text{ ksf}}$$

Reduction in Soil Pressure Due to Vertical Earthquake = 2.12 (0.10g x 0.4) = 0.08 ksf

Reduction in Soil Pressure Due to Bottom Pressure Moment (see Sections 2.2.1 and 3.2)

$$= \frac{1}{2} \frac{4930(25)}{\pi(26)^4/4} = \underline{0.17 \text{ ksf}}$$

Total Soil Pressure = 2.12 - 0.08 - 0.17 = 1.87 ksf

Uplift Moment = $(1.87)(4)\pi(26)^2$ = 15885 k-ft

Factor of Safety Against Uplift of the Foundation = $\frac{15885}{8154}$ = 1.95

FIGURE VI-4-2. FOUNDATION UPLIFT

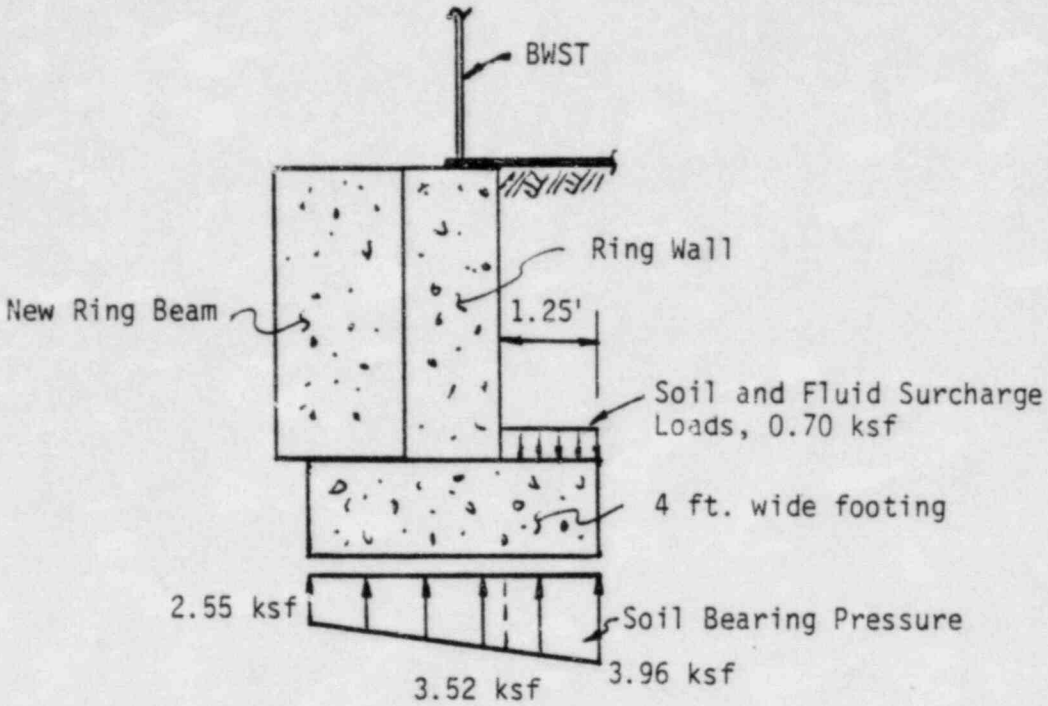

a) Soil Bearing on Footing

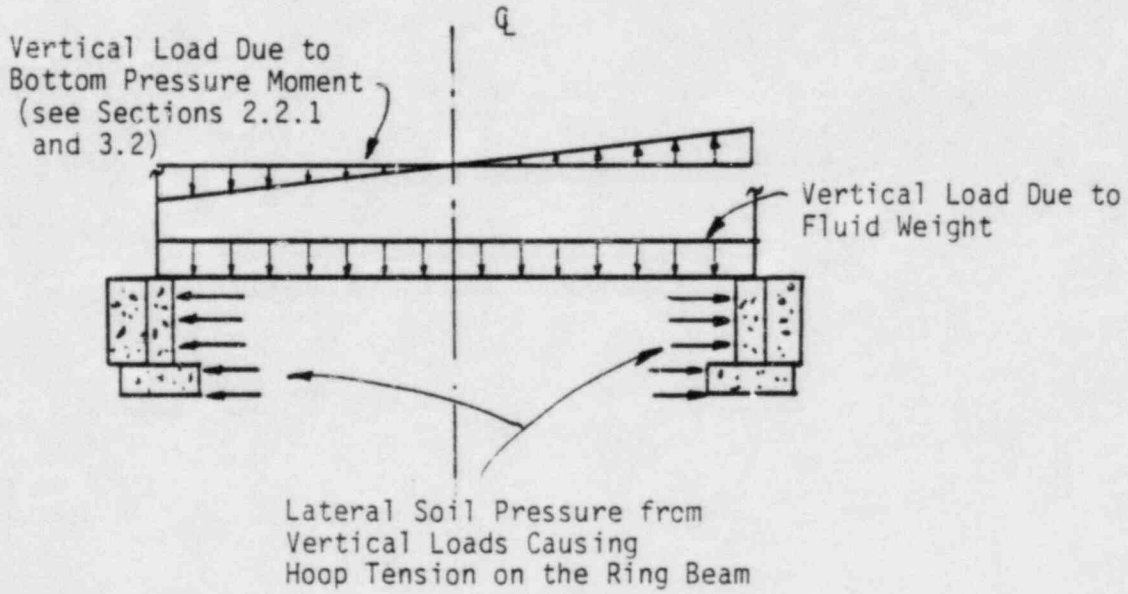

b) Hoop Tension on the Foundation

FIGURE VI-4-3. RING WALL LOADING CONDITIONS

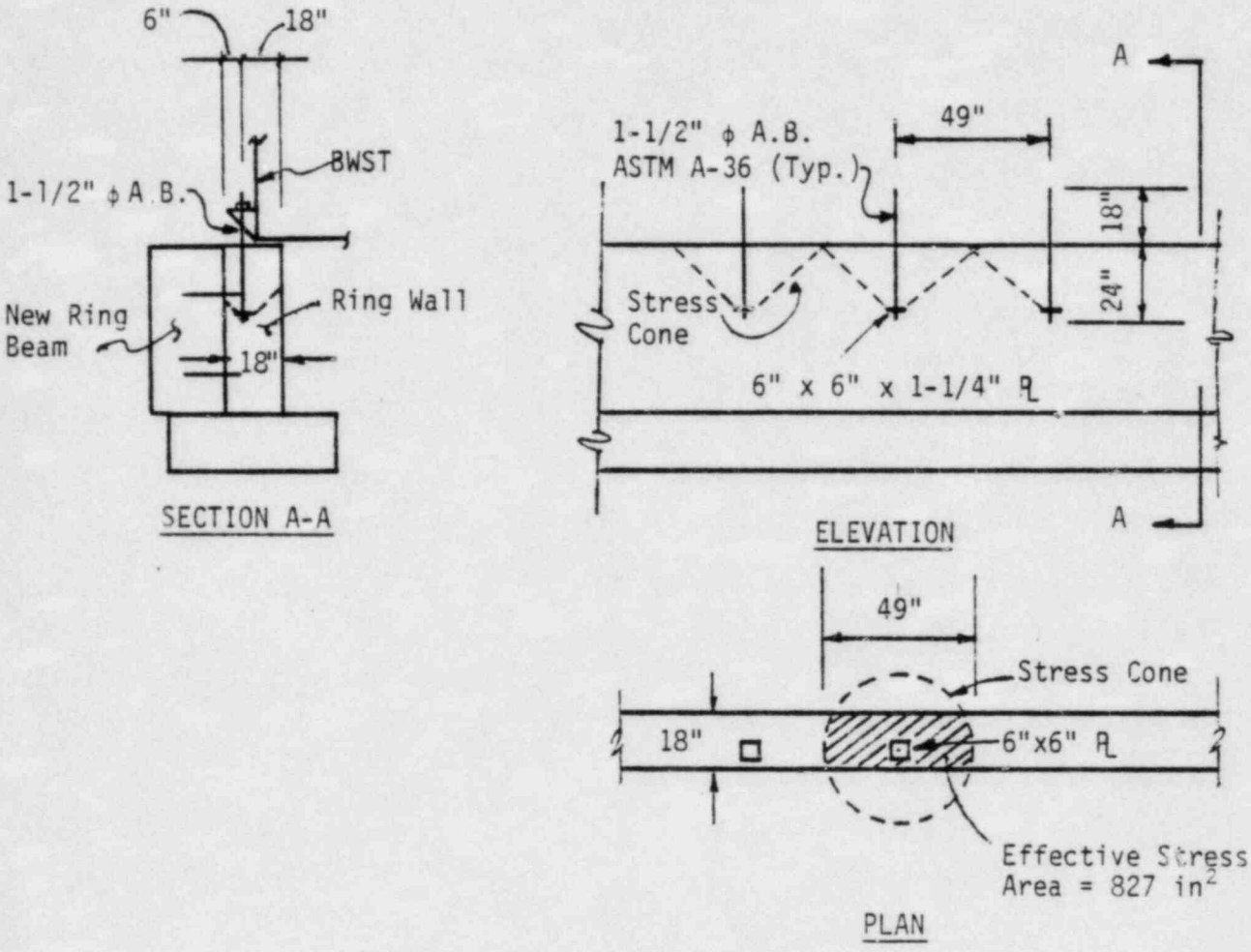

$$\text{Concrete Strength} = 4\phi\sqrt{f'_c}$$

$$\text{Pullout Capacity} = \text{Concrete Strength} \star \text{Effective Stress Area}$$

$$= \frac{4\times(0.65)\sqrt{4000}\times 827}{1000}$$

$$= 136 \text{ kips}$$

FIGURE VI-4-4. BWST ANCHOR BOLT PULLOUT CAPACITY

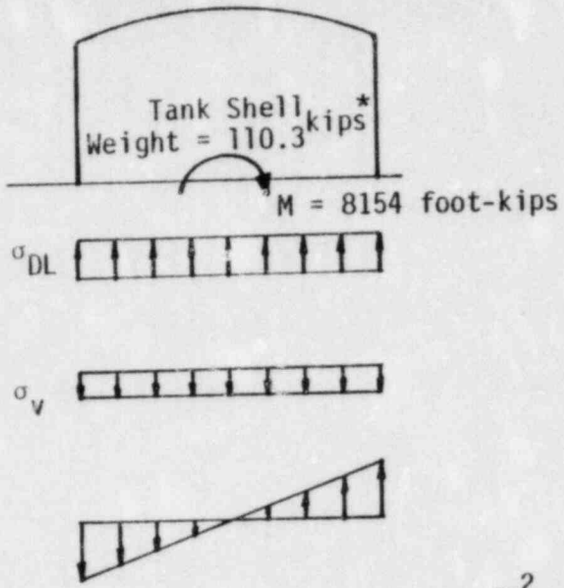

Area of 3/8 inch shell = $5.1\ ft^2$

Section modulus of 3/8 inch

Shell = $66.4\ ft^3$

* NOTE: Use 90 percent of the tank weight in accordance with ACI 349-80 since dead load is beneficial to bolt force

$\therefore W_S = 0.9(110.3) = 99.3$ kips

Maximum Bolt Force, $F_B = \sigma_t\ t\ell_t$

where

σ_t = tensile stress in the tank shell due to seismic-induced overturning moment, M

t = shell thickness = 3/8 inch

ℓ_t = portion of tank circumference tributary to each anchor bolt = $\pi(52)/40 = 4.08'$

$$\sigma_t = \sqrt{\sigma_{ms}^2 + \sigma_v^2} - \sigma_{DL}$$

where

σ_{ms} = tensile stress due to M

σ_v = tensile stress due to vertical earthquake

σ_{DL} = compressive stress due to dead load*

$$\sigma_t = \sqrt{\left(\frac{8154}{66.4}\right)^2 + \left[\frac{(99.3)}{5.1}\ (.10)\right]^2} - \frac{99.3}{5.1} = 103.3\ ksf$$

$$F_B = 103.3(.375/12)(4.08) = 13.2\ kips$$

FIGURE VI-4-5. CALCULATION OF MAXIMUM ANCHOR BOLT FORCE

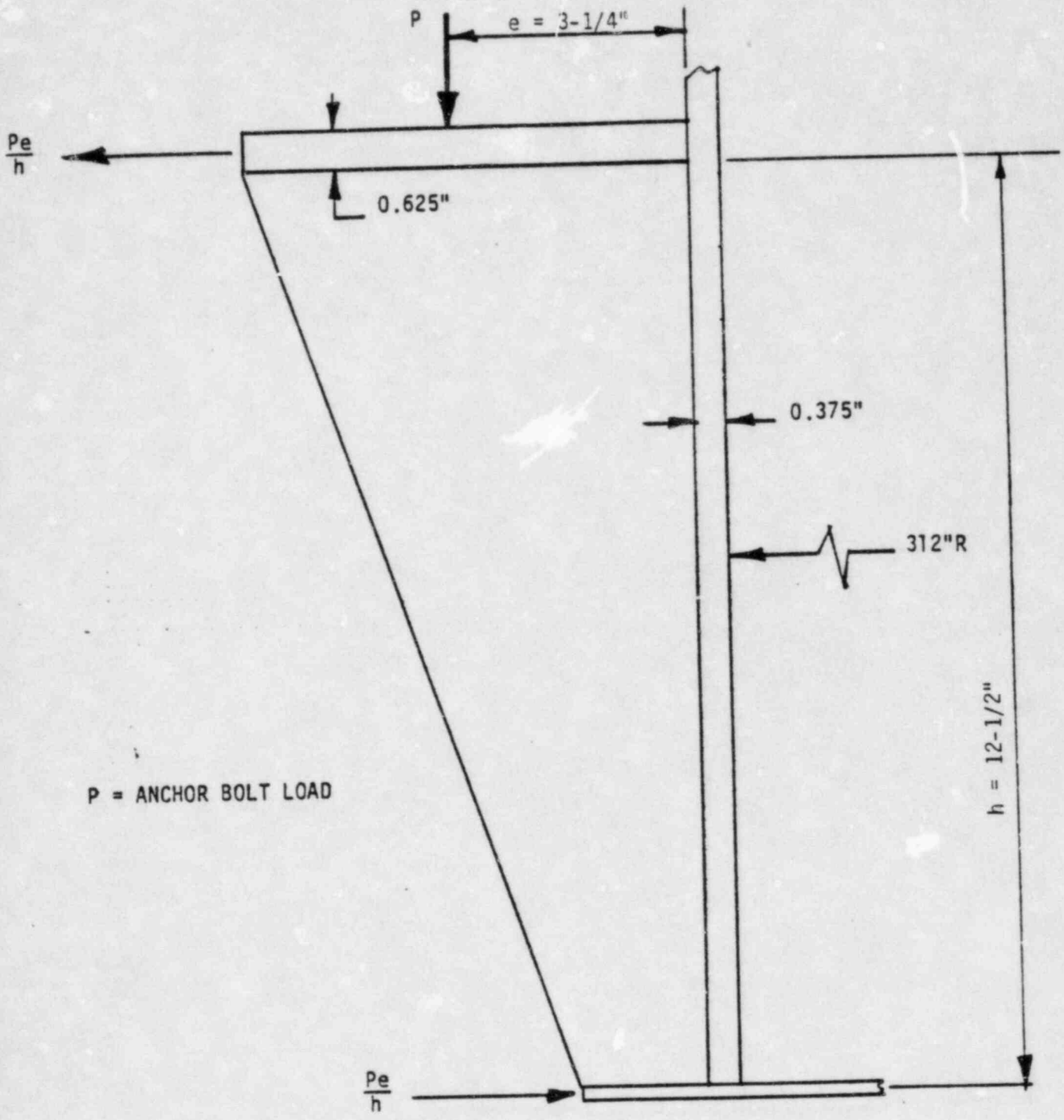

FIGURE VI-4-6. ANALYSIS MODEL FOR LOCAL MEMBRANE STRESSES IN SHELL DUE TO ANCHOR BOLT LOADING

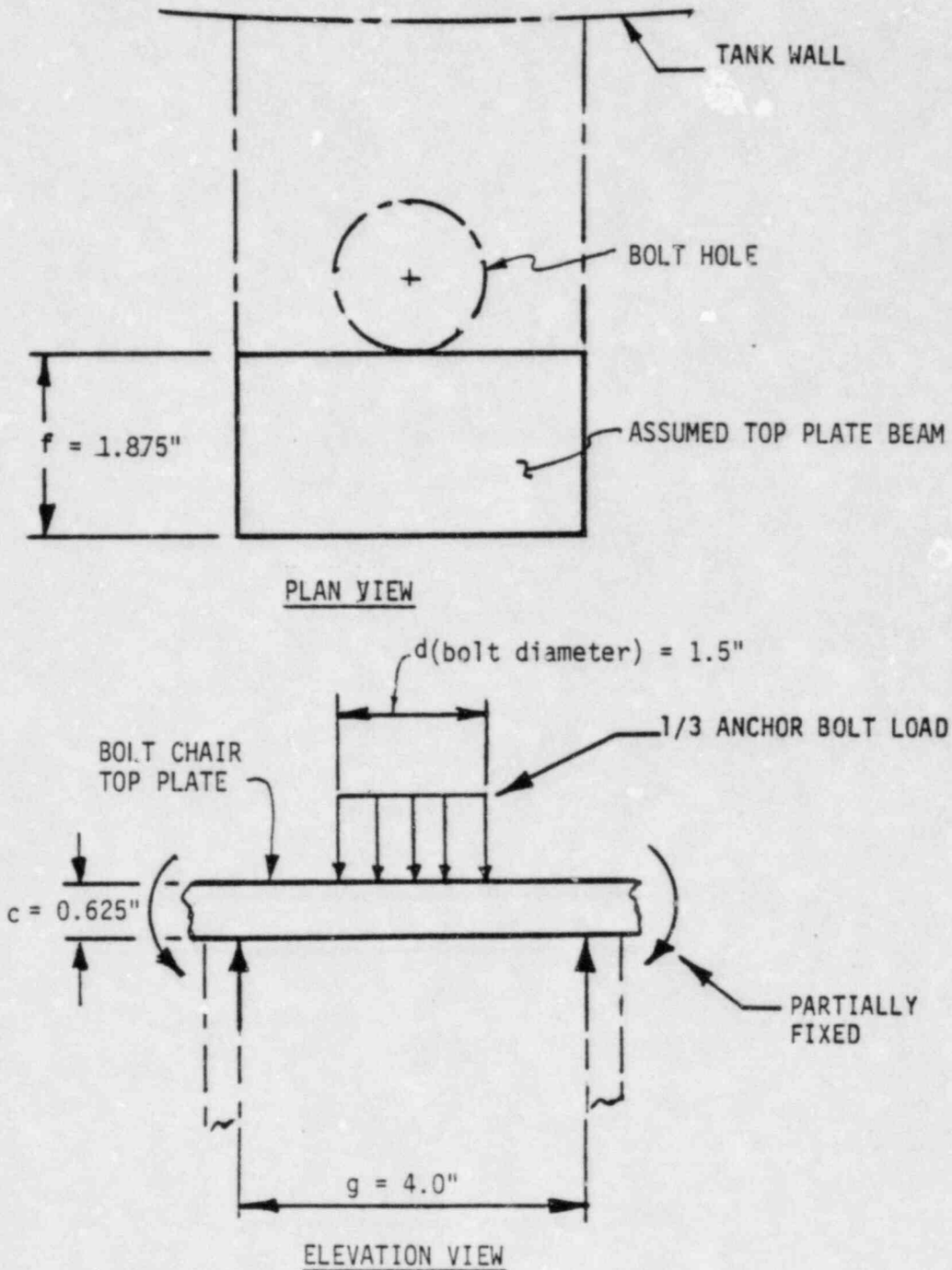

FIGURE VI-4-7. BEAM MODEL FOR BOLT CHAIR DESIGN
(Reference 14)

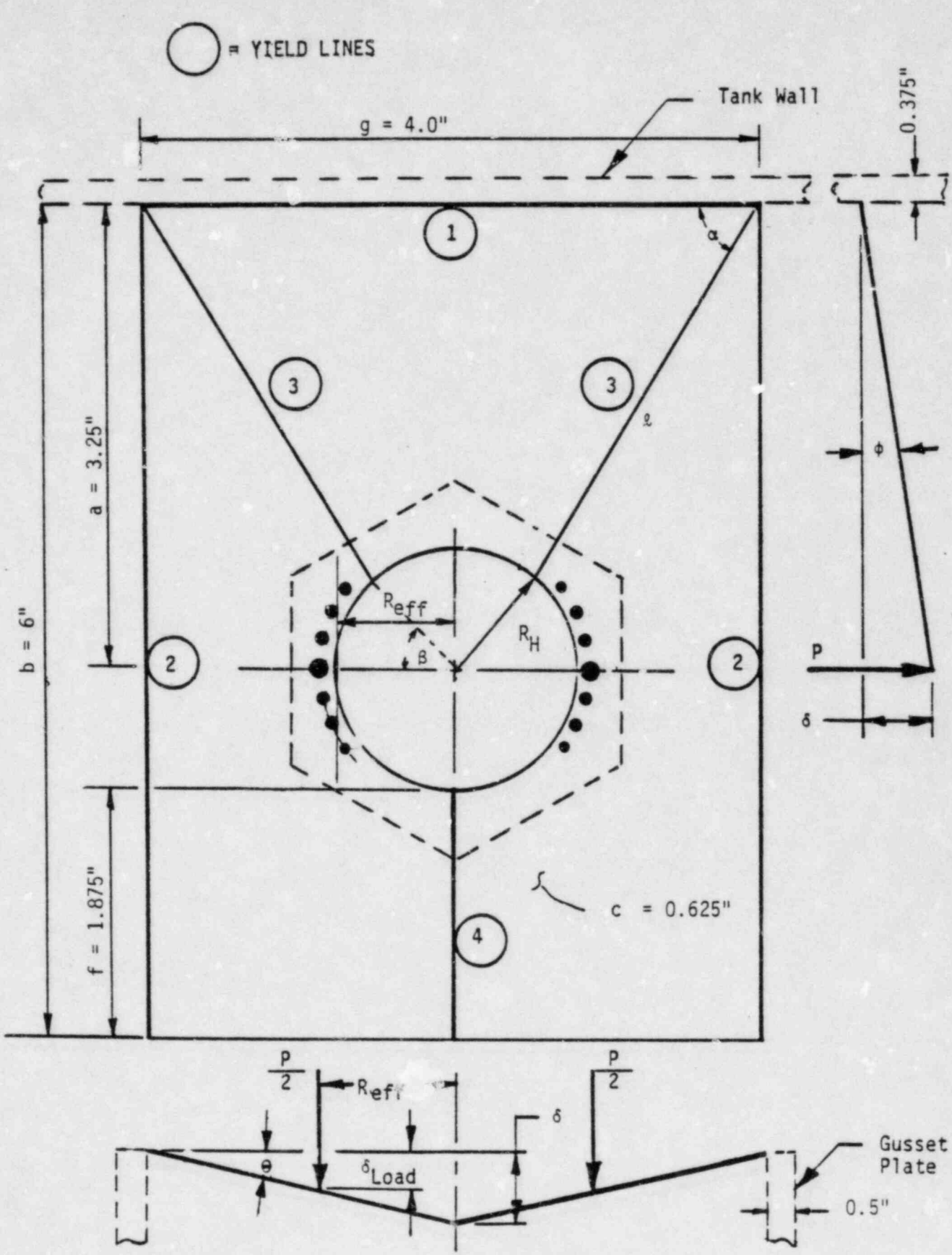

FIGURE VI-4-8. YIELD LINE MODEL FOR BOLT CHAIR

5. SUMMARY OF SME CODE MARGINS

The SME Code Margin (CM) and the multiplication factor (F_{SME}) by which the SME would have to be multiplied to raise stresses to code allowable levels are summarized in Table VI-5-1 for various elements. The lowest CM and F_{SME} reported in Table VI-5-1 are for the concrete foundation as discussed in Section 4.2.1. The F_{SME} value of 1.57 for the foundation was evaluated in an extremely conservative manner by scaling the margin from the governing foundation design check load combination which included 1.9 times the OBE by the ratio of 1.9 times the OBE overturning moment and the SME overturning moment. This process is extremely conservative because the foundation design check margin was predominantly affected by differential settlement and not by 1.9 OBE. It is demonstrated in Section 4.2.2.4, that the seismic margin factor, F_{SME}, of about 11 is more accurate for the concrete foundation. However, the CM and F_{SME} values in Table VI-5-1 are significantly over 1.0 and are based upon the detailed foundation design check analyses of the finite element representation of the ring wall, footing, ring beam and valve pit.

Other than for the concrete foundation, the lowest code margin reported in Table VI-5-1 is 1.50 associated with bolt chair uplift capacity. In this case, the SME would have to be multiplied by a factor of 1.69 to reach code capacity. Considering that the SME is a 0.15g earthquake, the earthquake that would be required to reach code allowable stresses in the BWST would have to be (0.15g)(1.69) or 0.25g.

The code margin capacity does not represent a failure capacity for the following reasons:

1. The Code Margins (CM) and SME multiplication factors (F reported in Table VI-5-1 are based upon the combination of the SME and conservative end-of-life settlement stresses. The full end-of-life settlement stresses are unlikely to exist during the SME. Furthermore, settlement stresses are displacement controlled stresses and are not expected to contribute to a failure during an earthquake. Even so, these stresses have been added to SME induced stresses.

2. The code capacities have built-in factors of safety. Thus, the actual failure capacities are substantially greater than the code capacities.

3. The stress and/or load parameters with the lowest code margins or F_{SME} do not directly contribute to failure of the tank. When the uplift capacity of the bolt chairs, or the uplift capacity of the foundation are exceeded, the tank will lift slightly. This lifting is not detrimental. In fact, many tanks are designed with no hold-down bolts because of the lack of consequences of uplift. All that uplift of one side of the tank does is to increase the compressive stresses on the opposite side.

4. The stress condition which most directly leads to tank failure is compressive buckling of the shell for which F_{SME} equals 2.44. In addition, considering that the shell compression is due to an overturning moment rather than uniform axial compression, the code capacity for compressive buckling contains a built-in factor of safety of 1.68 even under faulted condition allowables when compared with the buckling formula for bending based upon extensive static test data given in Reference 11. Even more relevant test data was recently published (Reference 18) for seismic shake table tests of cylindrical storage tanks. Buckling behavior during these tests would indicate that the code capacity for buckling with faulted condition allowables has a factor of safety of 2.98.

Considering these factors, the failure capacity earthquake for the BWST and its foundation is more than twice the 0.25g level at which code capacity is reached.

The BWST and its foundation easily pass the seismic margin earthquake check in all aspects.

TABLE VI-5-1

SME CODE MARGINS

(SME + DW + SETTLEMENT)

Stress or Load Parameter		CM	F_{SME}
Concrete Foundation		1.43	1.57*
Soil Bearing Capacity		1.57	2.28
Tank Sliding Capacity		2.5	2.5
Uplift Capacity of Foundation		1.95	1.75
Anchor Bolt Uplift Capacity		2.65	3.27
Bolt Chair Uplift Capacity		1.50	1.69
Tensile Hoop Stress	3/8" Shell	2.44	12.1
	1/4" Shell	2.13	8.40
Compressive Buckling Stress	3/8" Shell	2.22	3.74
	1/4" Shell	1.53	2.44
Local Membrane Stresses of Bolt Chair		1.71	2.89

* Very conservatively evaluated

6. REFERENCES

1. "Site Specific Response Spectra Midland Plant - Units 1 and 2, Part II - Response Spectra Applicable for the Top of Fill Material at the Plant Site", Weston Geophysical Corporation, Westboro, Massachusetts, May 1, 1981.

2. "Nuclear Reactors and Earthquakes", TID-7024, Prepared by Lockheed Aircraft Corporation and Holmes & Narver, Inc., for the Division of Reactor Development, U.S. Atomic Energy Commission, Washington, D.C., August, 1963.

3. USNRC Regulatory Guide 1.60, "Damping Values for Seismic Design of Nuclear Power Plants", October, 1973.

4. Veletsos, A. S., and Y. T. Wei, "Lateral and Rocking Vibration of Footings", ASCE Soil Mechanics Journal, SM9, September, 1971, pp. 1227-1248.

5. Kausel, E., and R. Ushijima, "Vertical and Torsional Stiffnesses of Cylindrical Footing", Massachusetts Institute of Technology, Department of Civil Engineering, Research Report R79-6, February, 1979.

6. Veletsos, A. S., "Seismic Effects in Flexible Liquid Storage Tanks", Proceedings of the International Association for Earthquake Engineering Fifth World Conference, Rome, Italy, 1974, Vol. 1, pp. 630-639.

7. Veletsos, A. S., and Yang, J. Y., "Dynamics of Fixed-Based Liquid-Storage Tanks", Presented at U.S.-Japan Seminar for Earthquake Engineering Research with Emphasis on Lifeline Systems, Tokyo, Japan, November, 1976.

8. Letter, Dr. D. P. Woods to Dr. S. S. Afifi, February 22, 1980, 10 CFR 50.54(f), Vol. 6, TAB 120.

9. "Final Safety Analysis Report, Midland Plant - Units 1 and 2", Consumers Power Company, 1981.

10. "Soil Dynamic Modulus Study, Midland Units 1 and 2, Consumers Power Company", Dames & Moore Job No. 05697-039-07, Dames & Moore, Park Ridge, Illinois, February, 1982.

11. NASA SP-8007, "Buckling of Thin-Walled Circular Cylinders", National Aeronautics and Space Administration, September, 1965.

REFERENCES (Continued)

12. "Design Report for the Borated Water Storage Tank Foundations - Consumers Power Company Midland Plant Units 1 and 2" transmitted to J. G. Keppler, U.S. Nuclear Regulatory Commission, Glen Ellyn, Illinois, from J. W. Cook, Consumers Power Company, Jackson, Michigan, November 13, 1981 and Addendum No. 1, November 24, 1981.

13. API 650, "Welded Steel Tanks for Oil Storage", Fifth edition and Supplement 1, October, 1973, American Petroleum Institute.

14. AISI Steel Plate Engineering Data - Vol. 2, "Useful Information on the Design of Plate Structures", Part VII, Anchor Bolt Chairs, February, 1979, American Iron and Steel Institute, Washington, D.C.

15. Campbell, R. D., et al, "Evaluation of Midland Nuclear Power Plant Borated Water Storage Tank for Non-Uniform Support Loading Resulting from Ring Wall Settlement", SMA 13704.01-R001 including Addenda, "Borated Water Storage Tank Analysis for End-of-Life Soil Settlement and Seismic Margin Earthquake Loading Conditions", Structural Mechanics Associates, Inc., Newport Beach, California, March, 1982.

16. Welding Research Council Bulletin 107, "Local Stresses in Spherical and Cylindrical Shells due to External Loadings", Welding Research Council, New York.

17. Hendron, A. J., Testimony to the Atomic Safety and Licensing Board, U.S. Nuclear Regulatory Commission, Consumers Power Company (Midland Plant, Units 1 and 2), Docket Nos. 50-329 OM, 50-330 OM, 50-329 OL, 50-330 OL, February, 1982.

18. Niwa, A. and R. W. Clough, "Buckling of Cylindrical Liquid Storage Tanks under Earthquake Loading", Earthquake Engineering and Structural Dynamics, Vol, 10, No. 1, pp. 107-122, John Wiley and Sons, January-February, 1982.

19. Structural Analysis and Design of Nuclear Plant Facilities, ASCE - Manuals and Reports on Engineering Practice - No. 58, American Society of Civil Engineers, pp 396- 397, New York, New York, 1980.

20. "Recommended Revisions to Nuclear Regulatory Commission Seismic Design Criteria", NUREG/CR-1161, Lawrence Livermore Laboratory, Livermore, California, December, 1979 (Draft) page 38.